were transferred to a *Il2rg*$^{-/Y}$ male (#122) with conditioning. Recipient #115 died 15 days after BM transfer (BMT), possibly due to conditioning toxicity, and recipient #605 died of presumptive pneumonia (not shown) 140 days posttransplantation; nevertheless, it survived longer than *Il2rg*$^{-/Y}$ controls without BMT, which died within 54 days. The remaining three recipients have survived >516 days (#610) and >321 days (#113 and #122) posttransplantation, with PB T cell populations exhibiting similar dynamics (Figures 2A and 2E); T cell counts increased ~6 weeks posttransplantation and remained high. Following early variability, PB B cell counts equilibrated at detectably low levels. The exception was #113, in which B cell counts were clearly higher than those of WT controls until 16 weeks posttransplantation, gradually decreasing thereafter to a level comparable with other recipients (Figures 2B and 2F). Compared to WT controls, recipient #610 PB contained similar T cell counts and a diminished but substantial number of B and NK cells 42 weeks posttransplantation (Figures 2A, 2B, and 2I). Similar profiles were observed in #113 and 122 (Figures 2E and 2F; not shown for NK). Surviving recipients and WT littermates had comparable granulocyte and monocyte numbers (Figures 2C, 2D, 2G, and 2H).

The provenance of immune cells in surviving recipients was examined by microsatellite marker analysis of genomic DNA from the ear, whole blood, and sorted T, B, and NK cells. GFP fluorescence of immune cells was also detected in the case of #122 (Figures 2E–2H and 2J). Lymphoid lineages were totally of donor origin in all recipients. Myeloid lineages were mainly of donor origin in #113 and of mixed donor/host origin in #122 and #610. Thus, our conditioning regimen enabled donor-derived myeloid lineage reconstitution in #113, but not #122. All surviving recipient PB contained IgG, IgA, and IgM (Figure 2K), albeit at varying levels, strongly suggesting that humoral immunity had been reconstituted and that donor-derived recipient B cells produced antibodies. Thus, allogeneic BM transplantation to *Il2rg*$^{-/Y}$ SCID pigs reproducibly resulted in enduring functional donor cell engraftment and reconstituted acquired immunity.

Assuming that the allogeneic model reported here reflects the behavior of cells transplanted from different species, SCID pigs promise to become a valuable tool in xenogeneic transplantation studies of human stem cells, such as hematopoietic, embryonic, and induced pluripotent stem cells (Takahashi et al., 2007). In particular, they promise to serve as platforms for the evaluation of therapeutic outcomes over several years, possibly after further genetic manipulation such as disruption of recombination activating genes 1 or 2 (*Rag1*, *Rag2*), which play critical roles in both cellular and humoral immunity (Shinkai et al., 1992) and may facilitate efficient human stem cell engraftment. Preliminary xenotransplantation of human BM cells to porcine *Il2rg*$^{-/Y}$ recipients in the absence of preconditioning permitted limited engraftment, underscoring the importance of further genetic manipulation, and optimized preconditioning (not shown). The porcine SCID model described here therefore represents an essential step toward the translational evaluation of human stem cells for long-term clinical applications.

SUPPLEMENTAL INFORMATION

Supplemental Information includes one figure, three tables, and Supplemental Experimental Procedures and can be found with this article online at doi:10.1016/j.stem.2012.04.021.

ACKNOWLEDGMENTS

This work was supported in part by a Grant-in-Aid from the Ministry of Agriculture, Forestry, and Fisheries of Japan. We thank staff in the Pig Management Section of the National Institute of Livestock and Grassland Science for assistance with animal management and Dr. T. Yagi for providing PKJ2 and MC1-DTA-p(A).

Received: November 17, 2011
Revised: March 13, 2012
Accepted: April 18, 2012
Published: June 13, 2012

REFERENCES

Asao, H., Okuyama, C., Kumaki, S., Ishii, N., Tsuchiya, S., Foster, D., and Sugamura, K. (2001). Cutting edge: the common gamma-chain is an indispensable subunit of the IL-21 receptor complex. J. Immunol. *167*, 1–5.

Cao, X., Shores, E.W., Hu-Li, J., Anver, M.R., Kelsall, B.L., Russell, S.M., Drago, J., Noguchi, M., Grinberg, A., Bloom, E.T., et al. (1995). Defective lymphoid development in mice lacking expression of the common cytokine receptor gamma chain. Immunity *2*, 223–238.

Felsburg, P.J., Hartnett, B.J., Henthorn, P.S., Moore, P.F., Krakowka, S., and Ochs, H.D. (1999). Canine X-linked severe combined immunodeficiency. Vet. Immunol. Immunopathol. *69*, 127–135.

Fischer, A., Cavazzana-Calvo, M., De Saint Basile, G., DeVillartay, J.P., Di Santo, J.P., Hivroz, C., Rieux-Laucat, F., and Le Deist, F. (1997). Naturally occurring primary deficiencies of the immune system. Annu. Rev. Immunol. *15*, 93–124.

Giri, J.G., Ahdieh, M., Eisenman, J., Shanebeck, K., Grabstein, K., Kumaki, S., Namen, A., Park, L.S., Cosman, D., and Anderson, D. (1994). Utilization of the beta and gamma chains of the IL-2 receptor by the novel cytokine IL-15. EMBO J. *13*, 2822–2830.

Ishii, N., Takeshita, T., Kimura, Y., Tada, K., Kondo, M., Nakamura, M., and Sugamura, K. (1994). Expression of the IL-2 receptor gamma chain on various populations in human peripheral blood. Int. Immunol. *6*, 1273–1277.

Ishikawa, F., Yasukawa, M., Lyons, B., Yoshida, S., Miyamoto, T., Yoshimoto, G., Watanabe, T., Akashi, K., Shultz, L.D., and Harada, M. (2005). Development of functional human blood and immune systems in NOD/SCID/IL2 receptor γ chain$^{(null)}$ mice. Blood *106*, 1565–1573.

Jiang, L., Lai, L., Samuel, M., Prather, R.S., Yang, X., and Tian, X.C. (2008). Expression of X-linked genes in deceased neonates and surviving cloned female piglets. Mol. Reprod. Dev. *75*, 265–273.

Kanai, N., Yanai, F., Hirose, S., Nibu, K., Izuhara, K., Tani, T., Kubota, T., and Mitsudome, A. (1999). A G to A transition at the last nucleotide of exon 6 of the gamma c gene (868G→A) may result in either a splice or missense mutation in

(I) Identification of immune subsets in recipient *Il2rg*$^{-/Y}$ male, #610, 12 weeks posttransfer as CD45RA$^+$CD3$^-$ B cells, CD3$^+$CD45RA$^+$ naive T cells, CD3$^+$CD45RA$^-$ memory T cells, and CD3$^-$CD16$^+$ NK cells among nonmyeloid and myeloid cells.
(J) Representative microsatellite PCR analyses to distinguish between donor and recipient DNA illustrated by the discriminatory marker (SW1263 for #610, SWR1367 for # 113, and SW24 for #122).
(K) Changes of IgG (left), IgA (middle), and IgM levels in serum from recipients (red lines) and wild-type controls (blue lines).

patients with X-linked severe combined immunodeficiency. Hum. Genet. *104*, 36–42.

Kimura, Y., Takeshita, T., Kondo, M., Ishii, N., Nakamura, M., Van Snick, J., and Sugamura, K. (1995). Sharing of the IL-2 receptor gamma chain with the functional IL-9 receptor complex. Int. Immunol. *7*, 115–120.

Kondo, M., Takeshita, T., Ishii, N., Nakamura, M., Watanabe, S., Arai, K., and Sugamura, K. (1993). Sharing of the interleukin-2 (IL-2) receptor gamma chain between receptors for IL-2 and IL-4. Science *262*, 1874–1877.

Leonard, W.J. (1996). The molecular basis of X-linked severe combined immunodeficiency: defective cytokine receptor signaling. Annu. Rev. Med. *47*, 229–239.

Nakamura, Y., Russell, S.M., Mess, S.A., Friedmann, M., Erdos, M., Francois, C., Jacques, Y., Adelstein, S., and Leonard, W.J. (1994). Heterodimerization of the IL-2 receptor beta- and gamma-chain cytoplasmic domains is required for signalling. Nature *369*, 330–333.

Nelson, B.H., Lord, J.D., and Greenberg, P.D. (1994). Cytoplasmic domains of the interleukin-2 receptor beta and gamma chains mediate the signal for T-cell proliferation. Nature *369*, 333–336.

Nelson, B.H., McIntosh, B.C., Rosencrans, L.L., and Greenberg, P.D. (1997). Requirement for an initial signal from the membrane-proximal region of the interleukin 2 receptor gamma(c) chain for Janus kinase activation leading to T cell proliferation. Proc. Natl. Acad. Sci. USA *94*, 1878–1883.

Noguchi, M., Nakamura, Y., Russell, S.M., Ziegler, S.F., Tsang, M., Cao, X., and Leonard, W.J. (1993a). Interleukin-2 receptor gamma chain: a functional component of the interleukin-7 receptor. Science *262*, 1877–1880.

Noguchi, M., Yi, H., Rosenblatt, H.M., Filipovich, A.H., Adelstein, S., Modi, W.S., McBride, O.W., and Leonard, W.J. (1993b). Interleukin-2 receptor gamma chain mutation results in X-linked severe combined immunodeficiency in humans. Cell *73*, 147–157.

Nolen, L.D., Gao, S., Han, Z., Mann, M.R., Gie Chung, Y., Otte, A.P., Bartolomei, M.S., and Latham, K.E. (2005). X chromosome reactivation and regulation in cloned embryos. Dev. Biol. *279*, 525–540.

Ohbo, K., Suda, T., Hashiyama, M., Mantani, A., Ikebe, M., Miyakawa, K., Moriyama, M., Nakamura, M., Katsuki, M., Takahashi, K., et al. (1996). Modulation of hematopoiesis in mice with a truncated mutant of the interleukin-2 receptor gamma chain. Blood *87*, 956–967.

Perryman, L.E. (2004). Molecular pathology of severe combined immunodeficiency in mice, horses, and dogs. Vet. Pathol. *41*, 95–100.

Puck, J.M., Nussbaum, R.L., and Conley, M.E. (1987). Carrier detection in X-linked severe combined immunodeficiency based on patterns of X chromosome inactivation. J. Clin. Invest. *79*, 1395–1400.

Russell, S.M., Keegan, A.D., Harada, N., Nakamura, Y., Noguchi, M., Leland, P., Friedmann, M.C., Miyajima, A., Puri, R.K., Paul, W.E., et al. (1993). Interleukin-2 receptor gamma chain: a functional component of the interleukin-4 receptor. Science *262*, 1880–1883.

Senda, S., Wakayama, T., Yamazaki, Y., Ohgane, J., Hattori, N., Tanaka, S., Yanagimachi, R., and Shiota, K. (2004). Skewed X-inactivation in cloned mice. Biochem. Biophys. Res. Commun. *321*, 38–44.

Shimozawa, N., Ono, Y., Kimoto, S., Hioki, K., Araki, Y., Shinkai, Y., Kono, T., and Ito, M. (2002). Abnormalities in cloned mice are not transmitted to the progeny. Genesis *34*, 203–207.

Shinkai, Y., Rathbun, G., Lam, K.P., Oltz, E.M., Stewart, V., Mendelsohn, M., Charron, J., Datta, M., Young, F., Stall, A.M., et al. (1992). RAG-2-deficient mice lack mature lymphocytes owing to inability to initiate V(D)J rearrangement. Cell *68*, 855–867.

Shultz, L.D., Lyons, B.L., Burzenski, L.M., Gott, B., Chen, X., Chaleff, S., Kotb, M., Gillies, S.D., King, M., Mangada, J., et al. (2005). Human lymphoid and myeloid cell development in NOD/LtSz-scid IL2R gamma null mice engrafted with mobilized human hemopoietic stem cells. J. Immunol. *174*, 6477–6489.

Takahashi, K., Tanabe, K., Ohnuki, M., Narita, M., Ichisaka, T., Tomoda, K., and Yamanaka, S. (2007). Induction of pluripotent stem cells from adult human fibroblasts by defined factors. Cell *131*, 861–872.

Takeshita, T., Asao, H., Ohtani, K., Ishii, N., Kumaki, S., Tanaka, N., Munakata, H., Nakamura, M., and Sugamura, K. (1992). Cloning of the gamma chain of the human IL-2 receptor. Science *257*, 379–382.

Traggiai, E., Chicha, L., Mazzucchelli, L., Bronz, L., Piffaretti, J.C., Lanzavecchia, A., and Manz, M.G. (2004). Development of a human adaptive immune system in cord blood cell-transplanted mice. Science *304*, 104–107.

Watanabe, S., Iwamoto, M., Suzuki, S., Fuchimoto, D., Honma, D., Nagai, T., Hashimoto, M., Yazaki, S., Sato, M., and Onishi, A. (2005). A novel method for the production of transgenic cloned pigs: electroporation-mediated gene transfer to non-cultured cells and subsequent selection with puromycin. Biol. Reprod. *72*, 309–315.

Thrombosis Research 129 (2012) e36–e40

Contents lists available at SciVerse ScienceDirect

Thrombosis Research

journal homepage: www.elsevier.com/locate/thromres

Regular Article

Lack of association between serum paraoxonase-1 activity and residual platelet aggregation during dual anti-platelet therapy

Tsukasa Ohmori [a,*,1], Yuichiro Yano [b,1], Asuka Sakata [a,b], Tomokazu Ikemoto [b], Masahisa Shimpo [b], Seiji Madoiwa [a], Takaaki Katsuki [b], Jun Mimuro [a], Kazuyuki Shimada [b], Kazuomi Kario [b,2], Yoichi Sakata [a,*,2]

[a] Research Division of Cell and Molecular Medicine, Center for Molecular Medicine, Jichi Medical University School of Medicine, 3311–1 Yakushiji, Shimotsuke, Tochigi 329–0498, Japan
[b] Division of Cardiovascular Medicine, Department of Medicine, Jichi Medical University School of Medicine, 3311–1 Yakushiji, Shimotsuke, Tochigi 329–0498, Japan

ARTICLE INFO

Article history:
Received 3 August 2011
Received in revised form 18 October 2011
Accepted 30 October 2011
Available online 25 November 2011

Keywords:
antiplatelet agent
platelet pharmacology
coronary syndrome

ABSTRACT

High residual platelet aggregability during thienopyridine treatment occurs because of low levels of the active drug metabolite, and is associated with an increased rate of major adverse cardiovascular events. Recent findings suggest that paraoxonase-1 (PON1) is a major determinant for clopidogrel efficacy. The aim of this study was to assess the impact of serum PON1 activity on platelet aggregability in thienopyridine-treated patients. In 72 patients receiving treatment with aspirin and ticlopidine after acute coronary syndrome, various laboratory data including the formation of platelet aggregations induced by agonists were compared with serum PON1 activities, measured as paraoxonase and homocysteine thiolactone hydrolase (HTLase). Serum paraoxonase activity was significantly associated with HTLase activity ($R=0.4487$, $P<0.0001$). These PON1 activities were not correlated with any parameters for platelet aggregation, hypertension, sleep apnea, and diabetes mellitus. In contrast, serum PON1 activities seemed to be involved in cardiac function, with brain natriuretic peptide and ejection fraction being significantly correlated with serum HTLase activity ($R=-0.2767$, $P=0.0214$) and paraoxonase activity ($R=0.2558$, $P=0.0339$), respectively. Paraoxonase activity also demonstrated a significant association with increased levels of ankle-brachial index ($R=0.267$, $P=0.0255$). Serum PON1 activities did not influence platelet aggregability during treatment with thienopyridine. However, they might modulate cardiac function after acute coronary syndrome and progression of atherosclerosis.

Introduction

The concept of antiplatelet resistance, particularly poor responsiveness to thienopyridine, has received increasing attention in recent years because of its reported involvement in cardiovascular events after percutaneous coronary artery intervention (PCI) [1-3]. Thienopyridines such as clopidogrel and ticlopidine are rapidly absorbed prodrugs, and must therefore be converted to an active metabolite to exert their inhibitory actions at the target $P2Y_{12}$ ADP nucleotide receptor on platelets. This conversion is *via* a two-step process involving the hepatic cytochrome P450 (CYP) enzyme pathway [4]. Resistance to clopidogrel was thought to result mainly from decreased CYP function leading to reduced active metabolite production [4]. Indeed, individuals carrying the loss-of-function polymorphism of the *CYP2C19* allele had significantly lower levels of the active metabolite of clopidogrel, and a higher rate of major adverse cardiovascular events [5,6]. Drug interaction with the CYP2C19 inhibitor, omeprazole, might also reduce the production of active metabolites [7,8].

Very recently, it was reported that paraoxonase-1 (PON1) is a major and essential factor in the production of active metabolites from clopidogrel [9]. PON1 hydrolyses 2-oxoclopidogrel (an oxidative metabolite of clopidogrel) to form the final active metabolite, a thiol derivative of clopidogrel (Supplemental Fig. 1) [9]. PON1 is a high-density lipoprotein-associated enzyme that prevents oxidative modification of low-density lipoprotein [10]. The *PON1* genotype (Q192 allele) has significant dose-dependent associations with decreased levels of serum PON1 activity and with increased levels of oxidative stress [11]. PON1 has multiple enzyme activities including paraoxonase, arylesterase, and thiolactonase (Supplemental Fig. 1). Although the full range of endogenous substrates hydrolysed by PON1 remains to be elucidated, PON1 has been shown to produce homocysteine from homocysteine thiolactone *via* its homocysteine thiolactone hydrolase (HTLase) activity [12].

Abbreviations: PON1, paraoxonase-1; HTLase, homocysteine thiolactone hydrolase; PCI, percutaneous coronary artery intervention; CYP, cytochrome P450; BNP, brain natriuretic peptide.

* Corresponding authors at: Research Division of Cell and Molecular Medicine, Center for Molecular Medicine, Jichi Medical University School of Medicine, 3111–1 Yakushiji, Shimotsuke, Tochigi 329–0498, Japan. Tel.: +81 285 58 7397; fax: +81 285 44 7817.
E-mail addresses: tohmori@jichi.ac.jp (T. Ohmori), yoisaka@jichi.ac.jp (Y. Sakata).

[1] TO and YY equally contributed in this study.
[2] KK and YS are co-senior authors due to equal contribution.

0049-3848/$ – see front matter © 2011 Elsevier Ltd. All rights reserved.
doi:10.1016/j.thromres.2011.10.033

We have previously investigated the mechanisms and clinical backgrounds that determine residual platelet aggregability, and attempted to ascertain whether platelet aggregability is involved in systemic thrombogenicity during dual antiplatelet therapy [13]. Using this previous population, we have retrospectively measured actual serum PON1 activities, measured as paraoxonase and HTLase, in 72 patients treated with ticlopidine and aspirin, and assessed the correlation between PON1 and platelet aggregability.

Methods

Patients

The institutional review board approved all study protocols, and informed consent was obtained from all participants. The design and protocol of this study has been described previously [13]. Briefly, we enrolled consecutive hospitalized patients from July 2006 to April 2007 who were treated by PCI because of symptomatic coronary artery disease. After normalization of cardiac enzymes, patients underwent blood sampling, ankle-brachial index monitoring and cardiorespiratory monitoring.

Blood collection and platelet aggregation

Platelet aggregation was assessed as described previously [14]. A fasting venous sample was carefully collected, and platelet-rich plasma was obtained by centrifugation. The aggregation response was measured based on the light scattering intensities obtained with a PA-200 platelet aggregation analyzer (Kowa Co. Ltd., Tokyo, Japan). This device is particularly sensitive for detecting and classifying the size of platelet aggregates (small, medium, and large) [14]. Platelet aggregation was stimulated with collagen (Hormon-Chemie, Munich, Germany), ADP (MC Medical Co., Tokyo, Japan) and thrombin receptor-activating peptide (TRAP; Invitrogen Co., Carlsbad, CA), a specific agonist for protease activating receptor-1. Blood samples (serum and plasma) were stored at −80 °C until analysis.

Laboratory testing

Plasma levels of plasminogen activator inhibitor-1 antigen, D-dimer, E-selectin and soluble fibrin were assayed using an automated latex agglutination assay (LPIA-S500; Mitsubishi Chemical Medience Co., Tokyo, Japan) based on conjugated monoclonal antibodies. The concentrations of brain natriuretic peptide (BNP) (ShionoRIA BNP kit; Shionogi USA, Inc. Florham Park, NJ) were measured by SRL Inc. (Tokyo, Japan).

Measurement of serum PON1 activities

We quantified paraoxonase and HTLase activities as a measure of serum PON1 activity (Supplemental Fig. 1). Serum paraoxonase activity was measured by using paraoxon as a substrate (Fully Automated Paraoxonase Activity Measurement Kit, Rel Assay Diagnostics, Gaziantep, Turkey). HTLase activity was measured by a hydrolysis of γ-thiobutyrolactone (Alfresa Auto HTLase, Alfresa Pharma Corp., Osaka, Japan). HTLase hydrolyzes the lactone ring of the substrate γ-thiobutyrolactone, producing free thiols that are detected using Ellman's reagent (DTNB; 5,5'-dithiobis (2-nitrobenzoic acid)). Assay reproducibility was high (coefficient of variation was less than 6%).

Statistical analysis

Statistical analyses were performed using Prism v5 (GraphPad software, Inc, La Jolla, CA). The associations between the individual parameters were calculated using Spearman's correlation method. All reported P values are two-sided; a P value of less than 0.05 was considered to indicate statistical significance.

Results

Patients

Of the 85 patients from our previous study, we selected 72 patients taking 100 mg / day of aspirin and 200 mg / day of ticlopidine after acute coronary syndrome. Base line characteristics of the study population are summarized in Table 1.

Lack of correlation of serum PON1 activities with platelet aggregation

We initially examined serum PON1 activities (measured by paraoxonase and HTLase activity). As show in Fig. 1, serum HTLase activity, but not paraoxonase activity, appeared to be normally distributed across the study population (HTLase: 130.3 ± 36.7 U/L; paraoxonase: 62.65 ± 25.27 U/L). These PON1 activities were significantly correlated ($R = 0.4487$, $P < 0.0001$). To examine whether serum PON1 activities determine platelet aggregability during dual antiplatelet therapy, serum PON1 activities were compared with several parameters of platelet aggregation. However, none of these parameters was significantly associated with PON1 activities (Fig. 2 and Table 2).

Correlation between serum PON-1 activities and cardiac function

We next compared serum PON1 activities with parameters for hypertension, sleep apnea, diabetes mellitus, hyperlipidemia, blood coagulation, arteriosclerosis, and cardiac dysfunction. Using linear regression analysis, we determined that only HDL cholesterol and BNP were correlated with HTLase activity (Table 3). Paraoxonase activity was associated with triglyceride, D-dimer, ankle-brachial index, and ejection fraction (Table 3). The medication including use of diuretics, angiotensin II receptor blocker, angiotensin converting enzyme inhibitor, beta blocker, calcium channel blocker, or statin did not demonstrate a significant association with serum PON1 activities (Supplemental Table 1). These data suggest that decreased levels of PON1 activity might lead to the acceleration of atherosclerosis and cardiac dysfunction after acute coronary syndrome.

Table 1
Characteristics of the study population.

Variables	Total subjects (n = 72)
Age, years	62.15 ± 11.62
Men, n (%)	57 (80)
BMI, kg/m^2	25.11 ± 3.514
Systolic blood pressure (mmHg)	125.3 ± 21.08
Diastolic blood pressure (mmHg)	76.6 ± 11.28
Pulse rate (/min)	72.39 ± 14.59
Blood sugar (mg/dl)	118.3 ± 50.43
HbA1c (%)	6.76 ± 1.891
Triglyceride (mg/dl)	130.2 ± 53.01
Total cholesterol (mg/dl)	167.7 ± 36.77
LDL cholesterol (mg/dl)	100.4 ± 30.35
HDL cholesterol (mg/dl)	41.3 ± 12.72
CPK max (U/L)	2,194 ± 2,211
BNP (pg/ml)	151.4 ± 183.6
Concomitant medications	
Antiplatelet agents, n (%)	
Aspirin + Ticlopidine	72 (100)
Antihypertensive medication, n (%)	66 (91.7)
Statin, n (%)	55 (76.4)
NSAIDs, n (%)	0 (0)

Data for continuous variables are expressed as the mean ± SD. BMI, body mass index; LDL, low-density lipoprotein; HDL, high-density lipoprotein; BNP, brain natriuretic peptide; NSAID, non-steroidal anti-inflammatory drug.

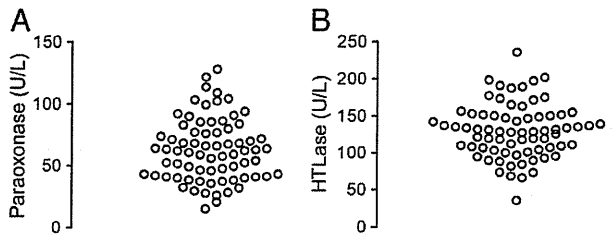

Fig. 1. Serum paraoxonase and HTLase activities in the study population.

Discussion

Inhibition of the $P2Y_{12}$ nucleotide receptor, an ADP receptor on platelets, is currently the gold-standard therapy for the prevention of ischemic events in patients undergoing PCI [15,16]. Although the second-generation thienopyridine, clopidogrel, is recommended by a number of current clinical guidelines, the inter-individual variability of its efficacy is a major drawback in its clinical use [17]. Better understanding of this variability in the efficacy of clopidogrel and other thienopyridines is vital at a time when the number of PCIs is increasingly rapidly. The loss-of-function polymorphism of the CYP2C19 allele has attracted attention as a potential factor in clopidogrel efficacy [4-6], while an elegant recent study suggested that PON1 is a major determinant in the production of the final active metabolite of clopidogrel [9]. In this study, we measured serum two PON1 activities in acute coronary syndrome and compared them with platelet aggregability in patients receiving dual antiplatelet therapy. We could identify no correlation between PON1 activities and any parameter for platelet aggregation in our population.

Several explanations may exist for the discrepancy between our result and the previous report. First, genetic divergence between

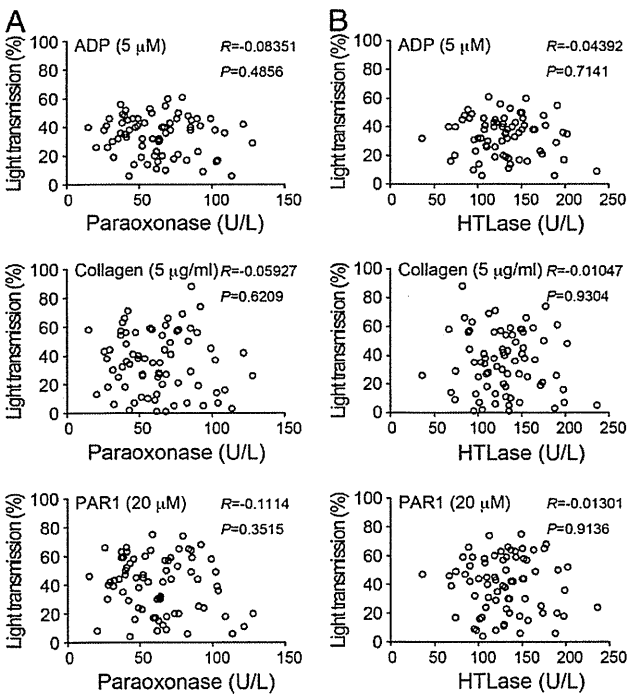

Fig. 2. Association between PON1 activities and platelet aggregation. Platelet aggregation induced by 5 μM ADP, or 5 μg / ml of collagen, or 20 μM TRAP was assessed by aggregometry, and was expressed as light transmission (%). Serum paraoxonase activities (U / L) (A) and HTLase activities (U / L) (B) were compared with platelet aggregation using Spearman's rank correlation coefficient.

Table 2
Correlation between serum paraoxonase activities and platelet aggregation.

	Paraoxonase		HTLase	
	R	*P* value	*R*	*P* value
ADP 2 μM-LT	−0.1252	0.2945	−0.03844	0.7486
ADP 2 μM-Small	−0.2083	0.0791	−0.07811	0.5143
ADP 2 μM- Med	−0.1335	0.2636	−0.01776	0.8823
ADP 2 μM-Large	−0.03798	0.7514	0.085	0.4777
ADP 5 μM-LT	−0.08351	0.4856	−0.04392	0.7141
ADP 5 μM-Small	−0.2212	0.0619	−0.09755	0.415
ADP 5 μM- Med	−0.2317	0.0501	−0.1055	0.3776
ADP 5 μM-Large	−0.1406	0.2389	−0.06589	0.5824
Coll 1 μg/ml-LT	−0.1072	0.37	0.02695	0.8222
Coll 1 μg/ml-Small	−0.1524	0.2012	0.06594	0.5821
Coll 1 μg/ml- Med	−0.1174	0.3262	0.04772	0.6906
Coll 1 μg/ml-Large	−0.00214	0.9857	0.04327	0.7182
Coll 5 μg/ml-LT	−0.05927	0.6209	−0.01047	0.9304
Coll 5 μg/ml-Small	−0.1489	0.212	−0.1001	0.4029
Coll 5 μg/ml- Med	−0.1269	0.2881	−0.03555	0.7669
Coll 5 μg/ml-Large	−0.1113	0.352	0.007927	0.9473
TRAP 20 μM-LT	−0.1114	0.3515	0.01301	0.9136
TRAP 20 μM -Small	−0.1585	0.1835	−0.1742	0.1434
TRAP 20 μM - Med	−0.09187	0.4427	−0.04854	0.6855
TRAP 20 μM -Large	−0.05235	0.6623	0.03127	0.7943

LT, light transmission; Small, small aggregates; Med, medium aggregates; Large, Large aggregates; Coll, collagen; TRAP, thrombin receptor-activating peptide (SFLLRN). *$P<0.05$.

Caucasian and Japanese patients might affect the result. The Japanese population is reported to express predominantly the 192R allele of *PON1* (192QQ: 18.2%; 192QR: 40.9%; 192RR: 40.9%) [18], whereas the Caucasian population in a large cohort study tended to express the 192Q variant (192QQ: 46.3%; 192QR: 43.9%; 192RR: 9.8%) [11]. The Q allele of *PON1* genotype was significantly and dose-dependently associated with decreased serum PON1 activity, whereby 192QQ, 192QR and 192RR had comparatively low, intermediate and high PON1 activity, respectively [11]. In contrast, the frequency of polymorphism for *CYP2C19*, a key enzyme in clopidogrel oxidation, varies among races, with loss-of-function polymorphisms reportedly being more common in Asian patients [19,20]. However, even in a genetically homogenous population, the *CYP2C19* allele was reported to account for only 12% of the variability in clopidogrel efficacy, whereas the *PON1*

Table 3
Correlation between paraoxonase activities and other laboratory data.

	Paraoxonase		HTLase	
	R	*P* value	*R*	*P* value
SBP	−0.0953	0.443	−0.118	0.3417
DBP	−0.121	0.3294	−0.00797	0.949
HR	−0.1096	0.3774	0.02895	0.8161
AHI	0.06843	0.5735	0.05563	0.6474
Blood suger	−0.06266	0.609	0.06714	0.5836
HbAlc	−0.08087	0.5121	−0.09806	0.4263
Triglyceride	0.2958	0.0129*	0.00273	0.9821
Total cholesterol	0.01199	0.9215	0.1166	0.3365
LDL cholesterol	−0.0158	0.8975	0.05602	0.6475
HDL cholesterol	−0.01299	0.915	0.2646	0.0269*
PAI-1	−0.08214	0.4928	0.01523	0.899
E-selectin	−0.0007075	0.9953	−0.1618	0.1746
Soluble Fibrin	−0.03224	0.788	−0.08483	0.4787
D-dimer	−0.2348	0.0471*	−0.2229	0.0598
max CPK	−0.1691	0.1616	−0.02521	0.8359
BNP	−0.1306	0.2849	−0.2767	0.0214*
Pulse wave velocity	−0.1665	0.1682	−0.04456	0.7141
ABI	0.267	0.0255*	−0.01957	0.8722
Ejection fraction	0.2558	0.0339*	0.1632	0.1803

SBP, systolic blood pressure; DBP, diastolic blood pressure; AHI, apnea-hypopnea index; LDL, low-density lipoprotein; HDL, high-density lipopurotein; PAI-1, plasminogen activator inhibitor-1; BNP, brain natriuretic peptide; ABI, ankle-brachial index. *$P<0.05$.

Q192R polymorphism was estimated to be responsible for 72.5% of the variability in ADP-stimulated platelet aggregation after clopidogrel administration [9]. It is therefore important that we clarify which polymorphism combinations (of *PON1* and *CYP2C19*) are the most relevant in the metabolism of thienopyridines in our population.

The first-generation thienopyridine, ticlopidine, was used instead of clopidogrel in our study because ticlopidine was the only approved drug for acute coronary syndrome in Japan during our study period. We acknowledge the possibility that the rate-limiting enzyme for ticlopidine metabolism to its active metabolite may differ from that of clopidogrel. All thienopyridines including ticlopidine, clopidogrel, and prasugrel are prodrugs that need to be converted into active metabolite through the formation of thiolactone metabolites (2-oxo-ticlopidine, 2-oxo-cloipdogrel, and prasugrel thiolactone, respectively (see Supplemental Fig. 1)) [4]. The free active thiol of these active metabolites forms disulfide bonds with, and therefore binds irreversibly to, cysteine residues Cys17 and Cys270 of $P2Y_{12}$ [21]. It is of great importance, therefore, to understand whether thiolactone metabolites of all thienopyridines are hydrolyzed mainly by PON1, or are instead oxidized by CYP.

We found correlations between PON1 activities and cardiac function in our study population. PON1 has a protective effect against oxidation of lipoproteins, and a *PON1* polymorphism (the 192Q allele) that produces decreased levels of PON1 activity was associated with systemic oxidative stress and higher rates of major cardiovascular events [11]. It is possible that decreased levels of PON1 activities enhance the progression of atherosclerosis in the coronary artery, resulting in decreased cardiac function after acute coronary syndromes. Indeed, reduced paraoxonase activity was significantly associated with a decreased ankle-brachial index in our study. Further studies are needed to assess the possible mechanisms and biological effect of PON1, particularly the severity of its effects on cardiac function after coronary artery disease.

Some limitations in this study merit discussion. First, we could assess platelet function testing in the patients treated with ticlopidine, but not clopidogrel. We cannot exclude the possibility that results may differ with other thienopyridines, as described above. In addition, we assessed only the correlation between serum PON1 activities and platelet response to ticlopidine, and we did not assess gene polymorphisms. Although it is accepted that serum PON1 activities are determined by *PON1* polymorphism, more data regarding genetic variation in *CYP* and *PON1* may have extended our findings relating to the mechanism(s) of the platelet response during dual antiplatelet therapy. Finally, the analysis reported here is *post hoc* analysis of a previously reported population and the number of participants is limited. We previously estimated that at least 62–85 participants would be required for the study ($\alpha = 0.05$, $\beta = 0.20$, and expected correlation coefficient, $R = 0.30$–0.35) [13]. Weak association due to β-error may affect the strength of any conclusions based on these data.

Conclusions

The current study has demonstrated that serum PON1 activities did not influence platelet aggregation in patients receiving thienopyridine treatment, but was involved in cardiac function. Our data suggest the need for a re-evaluation of the importance of PON1 (and/or CYP) in the production of active metabolites from thienopyridines. We may also need to consider how expression of the rate-limiting enzymes for thienopyridine metabolism differs between individual drugs and racial populations. During the preparation of this article, it was reported that no association exists between *PON1* genotype and platelet response to clopidogrel and stent thrombosis in a *post hoc* analysis of prospective studies [22]. Further large-scale prospective studies are required to determine which enzyme (PON1 or CYP) is critical for the production of active metabolites from thienopyridines, and therefore for cardiovascular events during thienopyridine administration.

Supplementary materials related to this article can be found online at doi:10.1016/j.thromres.2011.10.033.

Conflict of interests statement

T.O. has received financial support from Daiichi Sankyo. The other authors declare that they have no competing interest.

Acknowledgements

We would like to acknowledge Dr. Y. Yatomi (The University of Tokyo) for very helpful discussions. The authors are grateful for the hard work of the Coronary Care Unit staff in patient recruitment and management. We also thank N. Matsumoto and M. Ito for their excellent technical assistance. This study was supported by grants from the Support Program for Strategic Research Infrastructure from the Japanese Ministry of Education, Culture, Sports, Science and Technology.

References

[1] Alexopoulos D. Clopidogrel pretreatment in PCI: absolute requirement or obsolete myth? Int J Cardiol 2011;146:305–10.
[2] Farre AJ, Tamargo J, Mateos-Caceres PJ, Azcona L, Macaya C. Old and new molecular mechanisms associated with platelet resistance to antithrombotics. Pharm Res 2010;27:2365–73.
[3] Maree AO, Fitzgerald DJ. Variable platelet response to aspirin and clopidogrel in atherothrombotic disease. Circulation 2007;115:2196–207.
[4] Cattaneo M. The platelet P2Y receptor for adenosine diphosphate: congenital and drug-induced defects. Blood 2011;117:2102–12.
[5] Mega JL, Close SL, Wiviott SD, Shen L, Hockett RD, Brandt JT, et al. Cytochrome p-450 polymorphisms and response to clopidogrel. N Engl J Med 2009;360:354–62.
[6] Simon T, Verstuyft C, Mary-Krause M, Quteineh L, Drouet E, Meneveau N, et al. Genetic determinants of response to clopidogrel and cardiovascular events. N Engl J Med 2009;360:363–75.
[7] Sibbing D, Morath T, Stegherr J, Braun S, Vogt W, Hadamitzky M, et al. Impact of proton pump inhibitors on the antiplatelet effects of clopidogrel. Thromb Haemost 2009;101:714–9.
[8] O'Donoghue ML, Braunwald E, Antman EM, Murphy SA, Bates ER, Rozenman Y, et al. Pharmacodynamic effect and clinical efficacy of clopidogrel and prasugrel with or without a proton-pump inhibitor: an analysis of two randomised trials. Lancet 2009;374:989–97.
[9] Bouman HJ, Schomig E, van Werkum JW, Velder J, Hackeng CM, Hirschhauser C, et al. Paraoxonase-1 is a major determinant of clopidogrel efficacy. Nat Med 2011;17:110–6.
[10] Goswami B, Tayal D, Gupta N, Mallika V. Paraoxonase: a multifaceted biomolecule. Clin Chim Acta 2009;410:1–12.
[11] Bhattacharyya T, Nicholls SJ, Topol EJ, Zhang R, Yang X, Schmitt D, et al. Relationship of paraoxonase 1 (PON1) gene polymorphisms and functional activity with systemic oxidative stress and cardiovascular risk. JAMA 2008;299:1265–76.
[12] Ferretti G, Bacchetti T, Marotti E, Curatola G. Effect of homocysteinylation on human high-density lipoproteins: a correlation with paraoxonase activity. Metabolism 2003;52:146–51.
[13] Yano Y, Ohmori T, Hoshide S, Madoiwa S, Yamamoto K, Katsuki T, et al. Determinants of thrombin generation, fibrinolytic activity, and endothelial dysfunction in patients on dual antiplatelet therapy: involvement of factors other than platelet aggregability in Virchow's triad. Eur Heart J 2008;29:1729–38.
[14] Ohmori T, Yatomi Y, Nonaka T, Kobayashi Y, Madoiwa S, Mimuro J, et al. Aspirin resistance detected with aggregometry cannot be explained by cyclooxygenase activity: involvement of other signaling pathway(s) in cardiovascular events of aspirin-treated patients. J Thromb Haemost 2006;4:1271–8.
[15] Becker RC, Meade TW, Berger PB, Ezekowitz M, O'Connor CM, Vorchheimer DA, et al. The primary and secondary prevention of coronary artery disease: American College of Chest Physicians Evidence-Based Clinical Practice Guidelines (8th Edition). Chest 2008;133:776S–814S.
[16] Wright RS, Anderson JL, Adams CD, Bridges CR, Casey Jr DE, Ettinger SM, et al. 2011 ACCF/AHA Focused Update of the Guidelines for the Management of Patients With Unstable Angina/Non-ST-Elevation Myocardial Infarction (Updating the 2007 Guideline) A Report of the American College of Cardiology Foundation/American Heart Association Task Force on Practice Guidelines Developed in Collaboration With the American College of Emergency Physicians, Society for Cardiovascular Angiography and Interventions, and Society of Thoracic Surgeons. J Am Coll Cardiol 2011;57:1920–59.
[17] Gurbel PA, Becker RC, Mann KG, Steinhubl SR, Michelson AD. Platelet function monitoring in patients with coronary artery disease. J Am Coll Cardiol 2007;50:1822–34.
[18] Togawa T, Mukai Y, Ohata K, Suzuki T, Tanabe S. Measurement of homocysteine thiolactone hydrolase activity using high-performance liquid chromatography with fluorescence detection and polymorphisms of paraoxonase in normal human serum. J Chromatogr B Analyt Technol Biomed Life Sci 2005;819:67–72.

[19] Kim KA, Song WK, Kim KR, Park JY. Assessment of CYP2C19 genetic polymorphisms in a Korean population using a simultaneous multiplex pyrosequencing method to simultaneously detect the CYP2C19*2, CYP2C19*3, and CYP2C19*17 alleles. J Clin Pharm Ther 2010;35:697–703.
[20] Jinnai T, Horiuchi H, Makiyama T, Tazaki J, Tada T, Akao M, et al. Impact of CYP2C19 polymorphisms on the antiplatelet effect of clopidogrel in an actual clinical setting in Japan. Circ J 2009;73:1498–503.
[21] Ding Z, Kim S, Dorsam RT, Jin J, Kunapuli SP. Inactivation of the human P2Y12 receptor by thiol reagents requires interaction with both extracellular cysteine residues, Cys17 and Cys270. Blood 2003;101:3908–14.
[22] Sibbing D, Koch W, Massberg S, Byrne RA, Mehilli J, Schulz S, et al. No association of paraoxonase-1 Q192R genotypes with platelet response to clopidogrel and risk of stent thrombosis after coronary stenting. Eur Heart J 2011;32:1605–13.

Haemophilia

Haemophilia (2012), 18, e323–e330 DOI: 10.1111/j.1365-2516.2011.02686.x

ORIGINAL ARTICLE *Laboratory science*

Immune response against serial infusion of factor VIII antigen through an implantable venous-access device system in haemophilia A mice

S. MADOIWA,* E. KOBAYASHI,† Y. KASHIWAKURA,* A. SAKATA,* A. YASUMOTO,* T. OHMORI,* J. MIMURO* and Y. SAKATA*

**Research Divisions of Cell and Molecular Medicine; and †Division of Development of Advanced Treatment, Center for Molecular Medicine, School of Medicine, Jichi Medical University, Shimotsuke, Tochigi, Japan*

Summary. Haemophilia A is a life long bleeding disorder caused by an inherited deficiency of factor VIII (FVIII). About 30% of haemophilia A patients develop neutralizing antibodies as a consequence of treatment with FVIII concentrates. Immune tolerance protocols for the eradication of inhibitors require daily delivery of intravenous FVIII. We evaluated the immune responses to serial intravenous administration of FVIII in preimmunized haemophilia A mice. We introduced an implantable venous-access device (iVAD) system into haemophilia A mice to facilitate sequential infusion of FVIII. After preimmunization with FVIII, the haemophilia A mice were subjected to serial intravenous administration of FVIII through the iVAD system. In all mice with serial infusion of FVIII, high titers of anti-FVIII inhibitory antibodies developed at 10 exposure days (EDs). However, the anti-FVIII IgG titers were decreased after 150 EDs of sequential low-dose infusion of FVIII [0.05 U g^{-1} body weight (BW) five times per week]. Proliferative response to *ex vivo* FVIII stimulation was significantly suppressed in splenic $CD4^+$ T cells from mice with serial low-dose FVIII infusion compared with those from mice with high-dose FVIII infusion (0.5 U g^{-1} BW five times per week) or preimmunized mice. Moreover, splenic $CD4^+$ T cells from mice with serial low-dose infusion of FVIII failed to produce interleukin-2 and interferon-γ. These data suggest that serial infusion of FVIII could induce T-cell anergy in haemophilia A mice with inhibitor antibodies.

Keywords: anergy, factor VIII, haemophilia A mice, inhibitor, venous-access device

Introduction

Haemophilia A is a life-long bleeding disorder caused by an inherited deficiency of factor VIII (FVIII) because of mutations in the FVIII gene [1]. About 30% of severe haemophilia A patients who received replacement therapy with intravenous FVIII products develop neutralizing antibodies that inhibit the function of substituted FVIII [2,3]. Once an inhibitor develops, treatment of bleeding episodes is quite difficult due to partial or complete lack of efficacy of replacement therapy. Immune tolerance induction (ITI) therapy using regular applications of FVIII is the only strategy that has been proven successfully to combine eradication of FVIII inhibitors and induction of FVIII-specific immune tolerance [2,4].

Central venous-access devices (VADs) are often used in haemophiliacs undergoing ITI to overcome difficulties of regular venous puncture [5,6]. The fully implantable devices offer many advantages compared with external catheters, because they generally have longer useful duration with lower rate of infectious complication and cannot be accidentally displaced [7]. Although ITI approach was introduced several decades ago, little is known about the immunological mechanisms that cause down-modulation of FVIII-specific immune responses and the induction of long-lasting immune tolerance against FVIII.

In this study we introduced an implantable VAD (iVAD) system into haemophilia A mice to facilitate serial intravenous infusion of FVIII and evaluated immune responses against FVIII in preimmunized haemophilia A mice. We demonstrated that sequential administration of FVIII through the iVAD system could induce T-cell anergy in adult haemophilia A mice with inhibitors.

Correspondence: Seiji Madoiwa, MD, PhD and Yoichi Sakata, MD, PhD, Research Division of Cell and Molecular Medicine, Center for Molecular Medicine, Jichi Medical University, 3311-1 Yakushi-ji, Shimotsuke, Tochigi 329-0498, Japan.
Tel.: +81 285 58 7398; fax: +81 285 44 7817;
e-mail: madochan@jichi.ac.jp

Accepted after revision 29 September 2011

Methods

Animal models

Haemophilia A mice (B6; $_{129}S_4$-F8^{tm1Kaz}/J) with targeted destruction of exon 16 of the FVIII gene were kindly provided by Dr H.H. Kazazian Jr (University of Pennsylvania, Philadelphia, PA, USA) [8]. All mice were housed and used in a pathogen-free facility at Jichi Medical University, Shimotsuke, Tochigi, Japan. All animal experiments were performed in accordance with regulations of the Japanese Council for Animal Care; Jichi Medical University Animal Care Committee approval all animal protocols.

iVAD system and intravenous injection of FVIII

Haemophilia A mice aged 12 weeks were anaesthetized by inhalation with 2.5% isoflurane in the anaesthesia unit (Univentor, ZTN 08, Malta). An iVAD system (SoloPort; Instech Laboratories, Plymouth Meeting, PA, USA) was placed into a pocket of back skin in the chest wall of each animal (Fig. 1). The catheter was then tunneled under the skin and introduced into the superior vena cava through a cut-down site of jugular vein under a zoom stereomicroscope (Nikon, Tokyo, Japan). The entire system was flushed with saline solution after insertion. Mice were infused with intravenous recombinant human FVIII formulated with sucrose (Kogenate FS; Bayer Healthcare, Leverkusen, Germany) through the iVAD system.

Assay for FVIII inhibitors

Inhibitory FVIII antibodies were measured according to the Bethesda assay [9]. In brief, mouse plasma was serially diluted in Owren's Veronal Buffer (Dade Behring, Deerfield, IL, USA), such that the remaining FVIII activity for each sample was between 25% and 75%, and mixed 1:1 with normal pooled human plasma at 37°C for 2 h. Residual human FVIII activity was measured by one-stage assay using 50 μL of FVIII-deficient human plasma (Kokusai-Shiyaku, Kobe, Japan) and a 50-μL sample from the previous incubation on a automated coagulometer (CA-500; Sysmex, Kobe, Japan). One BU mL^{-1} was defined as the dilution of plasma containing FVIII inhibitory activity that results in 50% inhibition of FVIII activity.

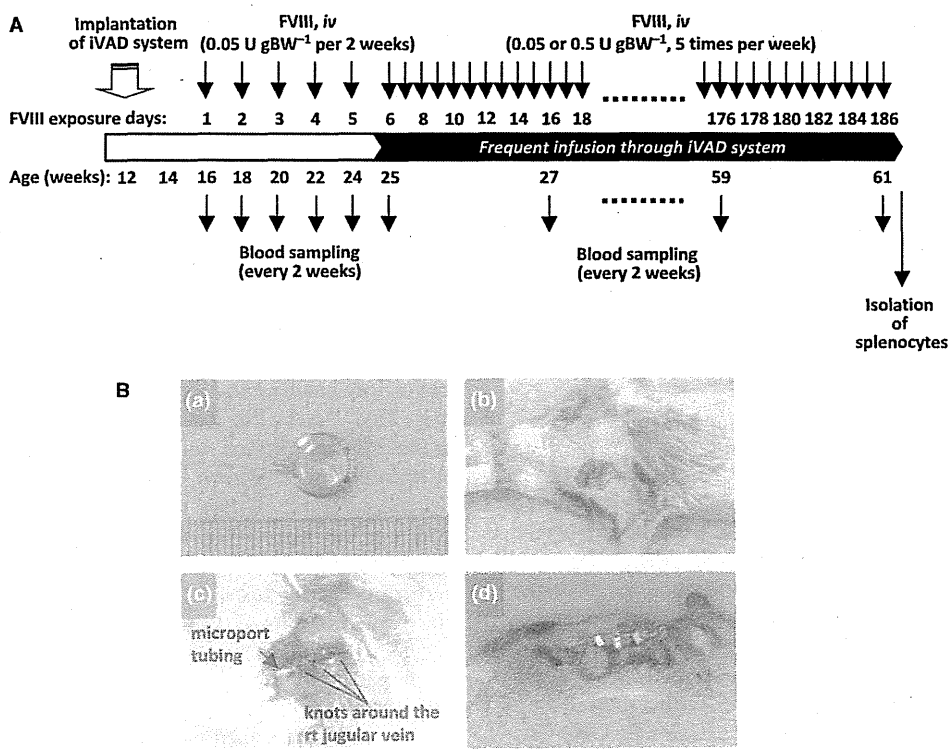

Fig. 1. Protocol for serial intravenous administration of FVIII through an implantable venous access device (iVAD) system in haemophilia A mice. A. Haemophilia A mice were implanted an iVAD system at age 12 weeks, then they were preimmunized with intravenous injection of 0.05 U g^{-1} BW recombinant human FVIII at 16, 18, 20, 22 and 24 weeks. After measurement of anti-FVIII inhibitory-antibodies titers, preimmunized mice were frequently administered with FVIII (0.05 or 0.5 U g^{-1} BW, five times per week) through the iVAD system. B. (a) The iVAD system consists of a stainless steel port with a molded silicon rubber and an 1.2 Fr catheter. After incision of the cervical skin in a haemophilia A mouse, the jugular vein was exposed (b), then the catheter was inserted into superior vena cava by cut-down procedure (c). The other side of the catheter was tunneled to the port that was set beneath the pocket of back skin (d).

Anti-FVIII measurement

Anti-FVIII IgG concentrations were determined by enzyme-linked immunosorbent assay (ELISA) in microtiter wells (Nunc, Roskilde, Denmark) coated with 1 μg mL^{-1} recombinant human FVIII. After blocking with 5% bovine serum albumin (BSA) in phosphate-buffered saline (PBS), serial dilutions of murine plasma were added at 4°C for 16 h. Each well was washed with 0.5% BSA in PBS containing 0.05% Tween-20. Horseradish peroxidase (HRP)-conjugated goat anti-mouse IgG (Cappel, Aurora, OH, USA) was added at 37°C for 1 h. ABTS Microwell substrate (KPL, Gaithersburg, MD, USA) was added, and the absorbance at 405 nm was read. Anti-FVIII antibody concentrations were calculated from the linear portion of a standard curve obtained using antihuman FVIII monoclonal antibodies (kindly provided by Chemo-Sero-Therapeutic Research Institute, Kumamoto, Japan).

Determination of anti-FVIII IgG subclasses

Microtiter wells were coated with 1 μg mL^{-1} recombinant human FVIII in PBS for 16 h at 4°C. After blocking with 5% BSA in PBS, serial dilutions of murine plasma were added for 2 h at 37°C. The wells were washed with 0.5% BSA in PBS containing 0.05% Tween-20. The IgG1, IgG2a, IgG2b and IgG3 subtypes of anti-FVIII antibodies bound to immobilized human FVIII were determined by incubation with isotype-specific rabbit anti-mouse IgGs (Mouse Typer; BioRad, Hercules, CA, USA) for 1 h at 37°C. After washing with 0.5% BSA in PBS containing 0.05% Tween-20, the wells were incubated with goat anti-rabbit HRP conjugate for 1 h at 37°C. Substrate development was performed for 15 min at 25°C, using ABTS Microwell substrate as described above.

Proliferation assay with [^{3}H]-thymidine incorporation

Mice splenic $CD4^+$ T cells were prepared by depletion of non-$CD4^+$ T cells with the autoMACS cell sorting system (Miltenyi Biotech GmbH, Bergisch Gladbach, Germany), according to the manufacturer's instructions. Antigen-presenting cells were prepared from mice splenocytes by depletion of T cells using the magnetic sorting system with anti-CD90 (Thy1.2)-conjugated microbeads (Miltenyi Biotech) followed by irradiation with a single dose of 20 Gy (Gamma Cell; Norton International, ON, Canada), to prevent non-specific proliferative responses during the *in vitro* FVIII stimulation assay. To measure T-cell proliferation, 3×10^5 $CD4^+$ T cells per well were cultured with 0–3 nM human recombinant FVIII in the presence of antigen-presenting cells derived from FVIII-immunized mice (five times injection of 0.05 U g^{-1} BW FVIII, every 2 weeks) at 37°C for 72 h in complete RPMI-1640 (Gibco BRL, Rockville, MD, USA). [^{3}H]-Thymidine (Amersham Bioscience, Uppsala, Sweden) was added (0.037 MBq per well) at 37°C for 18 h. Then, cells were harvested, and [^{3}H]-thymidine incorporation was determined by scintillation counting (Top count; Packard, Meriden, CT, USA).

Cytokine assays

Splenocytes were incubated in 24-well plates at 1.0×10^6 cells per well in the absence or presence of 3 nM human recombinant FVIII at 37°C in 5% CO_2. Production of interleukin (IL)-2, IL-4, IL-12 and interferon (IFN)-γ by $CD4^+$ T cells derived from each mouse was analyzed at 72 h by ELISA kits (Biotrak ELISA System; Amersham Biosciences, Piscataway, NJ, USA) according to the manufacturer's instructions. In addition, levels of IL-10 were measured at 96 h by ELISA system (Biotrak ELISA System).

Statistical analysis

Data are expressed as mean ± SE. Normally distributed variables were compared by Student's *t*-test. Variables not normally distributed were analyzed by two-sided Mann–Whitney U test. The data were considered statistically significant at P values < 0.05.

Results

Serial intravenous administration of FVIII through an iVAD system in preimmunized haemophilia A mice

We securely implanted venous access devices into haemophilia A mice at 12 weeks using a zoom microscopy, therefore, we could avoid using FVIII concentrates for haemostatic control during the procedure (Fig. 1B). After the operation-related wounds had healed, we developed immunized mice against FVIII by intravenous injection of FVIII (0.05 U g^{-1} BW) at 2-week intervals. Titers of anti-FVIII inhibitory antibodies of the mice were elevated to 100–400 BU mL^{-1} after the fifth exposure of FVIII. Thereafter, we performed serial infusion of FVIII into the preimmunized haemophilia A mice through the venous access device system. High titers (>2000 BU mL^{-1}) were developed after 10 exposure days (EDs) in mice with administration of FVIII (0.05 U g^{-1} BW five times per week) and were continued over 100–120 EDs. However, after 130–150 EDs their titers were gradually decreased despite continuing sequential stimulation of FVIII (Fig. 2a). One of the five mice was discontinued at 140 EDs because of bleeding from the site of catheter insertion (Fig. 2a; LD#3). In contrast, > 2000 BU mL^{-1} of anti-FVIII inhibitory antibodies were sustained over

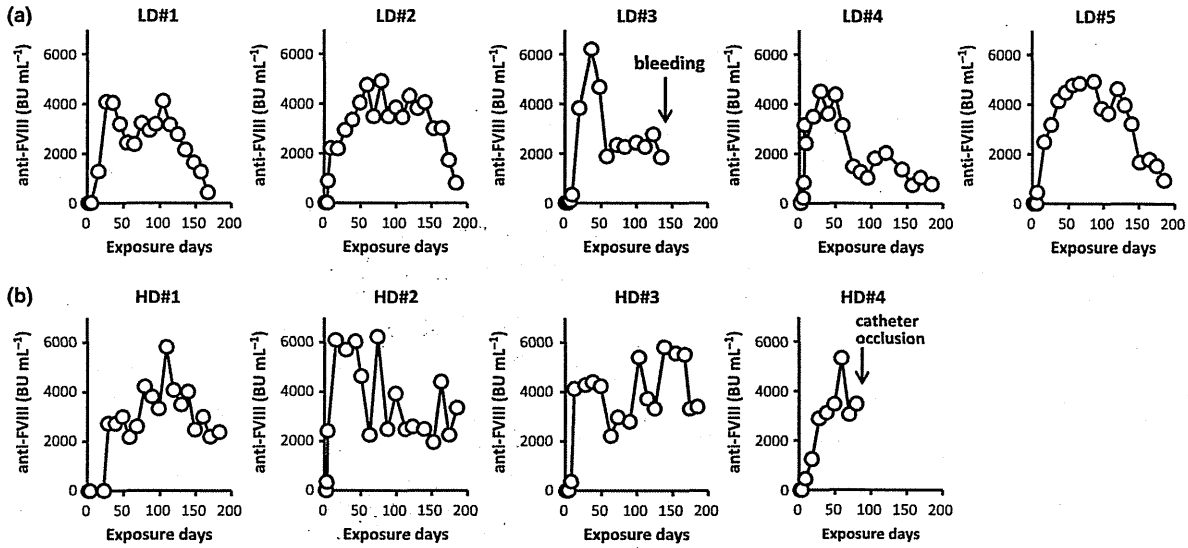

Fig. 2. Effect of serial intravenous administration of FVIII on anti-FVIII inhibitory antibody formation in preimmunized haemophilia A mice. Haemophilia A mice were intravenously immunized with 0.05 U g^{-1} BW FVIII at 16, 18, 20, 22 and 24 weeks. After measurement of anti-FVIII inhibitory-antibodies titers, preimmunized mice were frequently administered with FVIII [(a) 0.05 U g^{-1} BW five times per week; (b) 0.5 U g^{-1} BW, five times per week] through the iVAD system. The mice were bled at every 2 weeks, and their anti-FVIII inhibitor titers were determined by Bethesda assay.

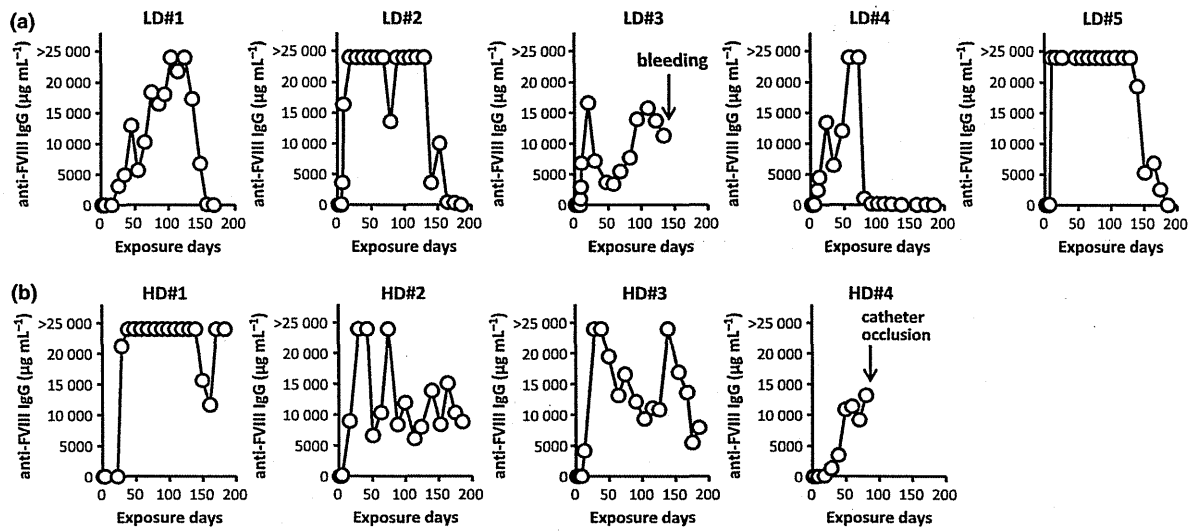

Fig. 3. Effect of repeated intravenous infusion of FVIII on FVIII-specific IgG formation in haemophilia A mice with inhibitors. Haemophilia A mice were intravenously immunized with 0.05 U g^{-1} BW FVIII at 16, 18, 20, 22 and 24 weeks. After measurement of anti-FVIII inhibitory-antibodies titers, pre-immunized mice were repeatedly infused with FVIII [(a), 0.05 U g^{-1} BW, five times per week; (b) 0.5 U g^{-1} BW, 5 times per week. The mice were bled at every two weeks just before each infusion. Plasma levels of FVIII-specific IgG were measured by ELISA as described in Methods.

180 EDs in mice with serial infusion of high-dose FVIII (0.5 U g^{-1} BW five times per week) (Fig. 2b).

Effect of serial intravenous infusion of FVIII on FVIII-specific IgG and subclasses formation

Anti-FVIII IgG was detectable immediately after serial infusion of FVIII (0.05 U g^{-1} BW five times per week) in preimmunized haemophilia A mice, and were persisted for more than 80–100 EDs (Fig. 3a). Interestingly, titers against FVIII were markedly decreased after 80–150 EDs. By contrast, preimmunized mice followed by serial intravenous infusion of high-dose FVIII (0.5 U g^{-1} BW five times per week) showed high titer of anti-FVIII IgG over 150–180 EDs (Fig. 3b). One of four mice receiving sequential high-dose FVIII infusion was discontinued due to occlusion of central vein catheter at 80 EDs (Fig. 3b; HD#4). All IgG isotypes of anti-FVIII IgG

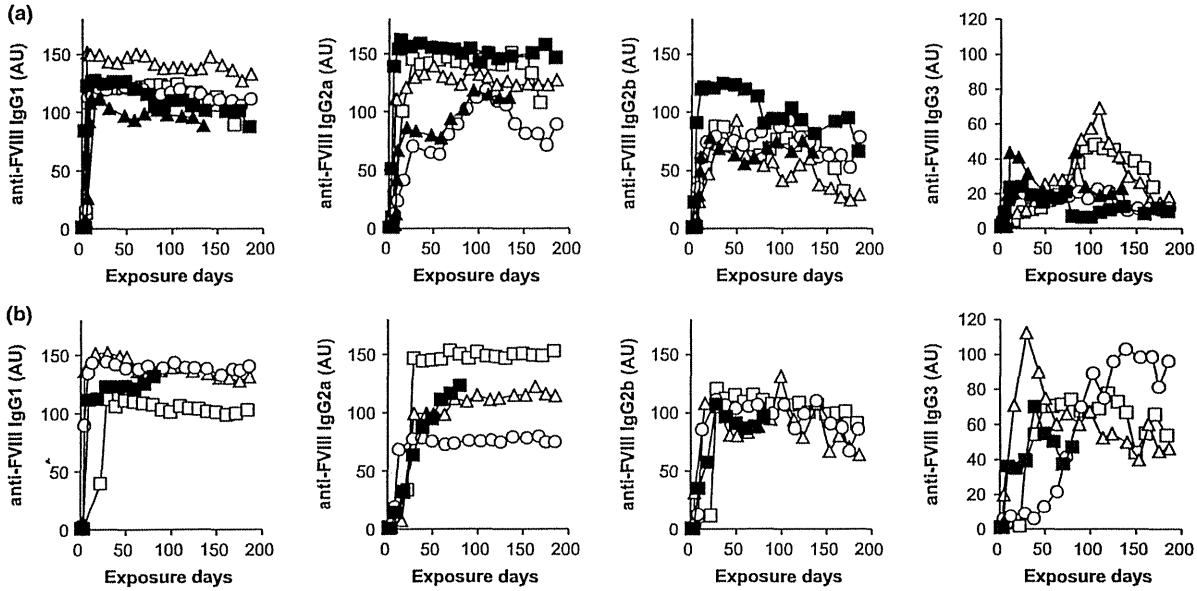

Fig. 4. Effect of serial intravenous injection on anti-FVIII IgG subclasses formation in preimmunized haemophilia A mice. (a) Haemophilia A mice (LD1, open squares; LD#2, open triangles; LD#3, closed triangles; LD#4, closed squares; LD#5, open circles) were intravenously immunized with 0.05 U g^{-1} BW FVIII at 16, 18, 20, 22 and 24 weeks. After measurement of anti-FVIII inhibitory antibodies titers, preimmunized mice were repeatedly infused with FVIII (0.05 U g^{-1} BW five times per week). (b) Haemophilia A mice (HD#1, open squares; HD#2, open triangles; HD#3, open circles; HLD#4, closed squares) were intravenously immunized with 0.05 U g^{-1} BW FVIII at 16, 18, 20, 22 and 24 weeks. After measurement of anti-FVIII inhibitory antibodies titers, preimmunized mice were repeatedly infused with FVIII (0.5 U g^{-1} BW five times per week). Each of the mice was bled at every two weeks just before FVIII infusion. Titers of IgG subclasses (IgG1, IgG2a, IgG2b and IgG3) were determined by ELISA as described in Methods.

antibodies were rapidly increased after serial infusion of 0.05 U g^{-1} and 0.5 U g^{-1} BW of FVIII (Fig. 4). However, in mice with repeated administration of 0.05 U g^{-1} BW FVIII titers of IgG3 subclass antibodies were decreased after 80–100 EDs (Fig. 4b).

Effect of serial administration of FVIII on anti-factor VIII CD4⁺ T cells proliferation

Next, we evaluated whether serial infusion of FVIII exerts a suppressive effect on FVIII-specific T cells, $CD4^+$ T cells obtained after the final injection were assayed for a T-cell proliferative response to FVIII. We observed a dose-dependent $CD4^+$ T-cell proliferative response to FVIII in preimmunized mice (five times injection of FVIII every two weeks, Fig. 5). In the group with sequential infusion of 0.5 U g^{-1} BW FVIII the T cells significantly proliferated in response to FVIII stimulation. By contrast, no response was observed at any FVIII dose in $CD4^+$ T cells from the mice after serial infusion of 0.05 U g^{-1} BW FVIII.

Effect of serial infusion of FVIII on cytokine response

Mice that were immunized with FVIII every two weeks developed splenocytes, which proliferated and produced

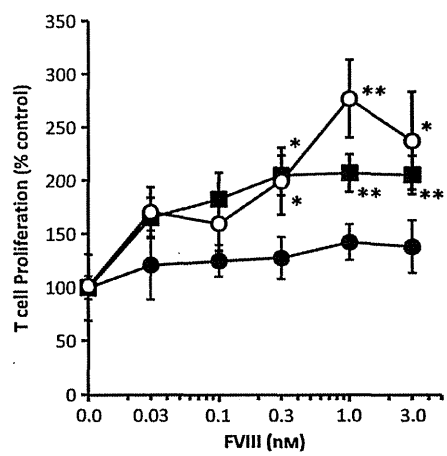

Fig. 5. Effect of repeated administration of FVIII on anti-factor VIII T-cell proliferation of haemophilia A mice. Haemophilia A mice were given intravenous injection of 0.05 U g^{-1} BW FVIII at 16, 18, 20, 22 and 24 weeks. After measurement of anti-FVIII inhibitory-antibodies titers, preimmunized mice were frequently infused with FVIII through the iVAD system. $CD4^+$ T cells of preimmunized mice (n = 5; open circles), mice with infusion of FVIII (0.05 U g^{-1} BW, five times per week; n = 4; closed circles), and mice with injection of FVIII (0.5 U g^{-1} BW, five times per week; n = 3; closed squares) were obtained three days after final immunization. The amount of ^{3}H-thymidine incorporation was measured under *in vitro* stimulation with FVIII (0–3 nM) in the presence of the FVIII-immunized mice-derived antigen-presenting cells by scintillation counting as described in the Methods. Data are means ± SD. $^*P < 0.05$; $^{**}P < 0.03$ when compared with the proliferation in the absence of FVIII.

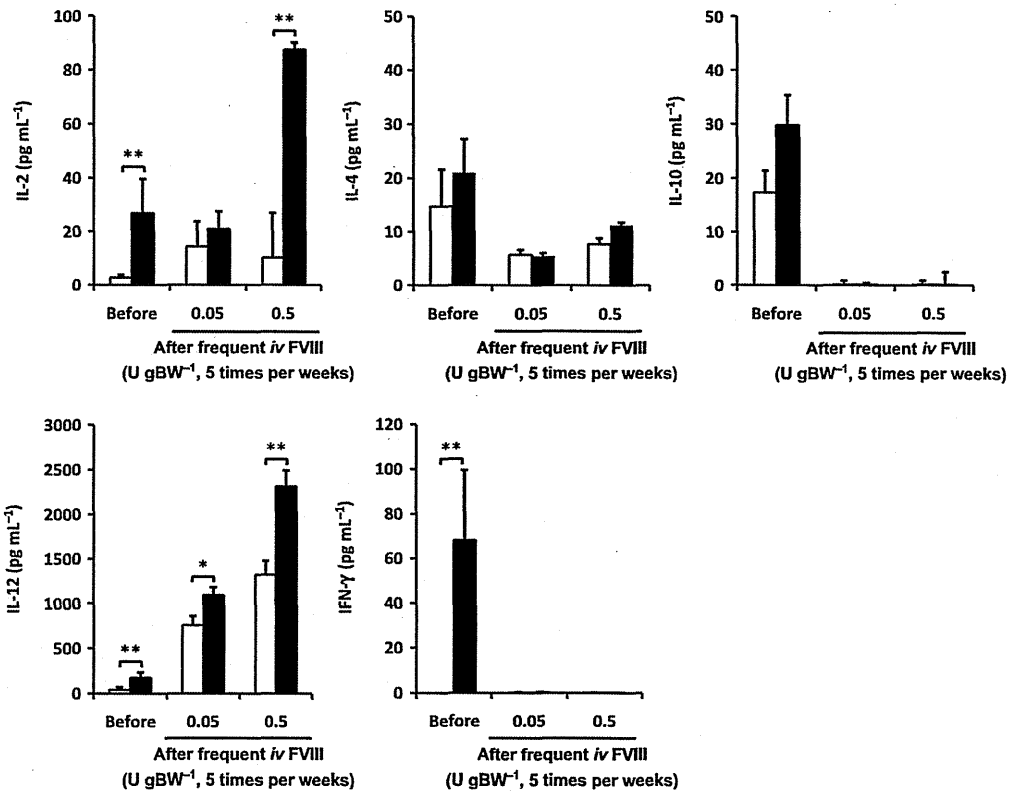

Fig. 6. Effect of serial infusion of FVIII on cytokine response of pre-immunized haemophilia A mice. Haemophilia A mice were intravenously immunized with 0.05 U g^{-1} BW FVIII at 16, 18, 20, 22 and 24 weeks. After measurement of anti-FVIII inhibitory antibodies titers, preimmunized mice were frequently administered with FVIII (0.05 or 0.5 U g^{-1} BW five times per week) through iVAD system. Splenocytes from pre-immunized (before, n = 5), frequently FVIII-infused [0.05 (n = 4) or 0.5 (n = 3) U g^{-1} BW five times per week] mice were cultured in the absence (open bars) or presence (closed bars) of 3 nM FVIII, and their cytokine production (IL-2, IL-4, IL-10, IL-12 and IFN-γ) were analyzed by ELISA as described in Methods. Values (pg mL^{-1}) are means ± SD. *P < 0.05; **P < 0.03.

IL-2, IL-12 and IFN-γ in response to *in vitro* FVIII stimulation (Fig. 6). In contrast, splenocytes deriving from mice with serial infusion of 0.05 U g^{-1} BW FVIII did not increase their production of IL-2 and IFN-γ, although they could secrete IL-12 after addition of FVIII. Moreover, 0.5 U g^{-1} BW FVIII-repeated administrated mice produced significant amounts of IL-2 and IL-12, but did not change IFN-γ levels even after stimulation of FVIII.

Discussion

Haemophilia A patients with inhibitors are infused daily FVIII according to immune tolerance protocols with the aim of eradicating the antibody [10,11]. Central VADs have been used to facilitate repeated administration of clotting factor concentrates in haemophiliac children requiring ITI [12,13]. We here established a method to implant a VAD into haemophilia A mice (Fig. 1). We could prevent exposure to FVIII antigen in the mice during the surgical procedure, because it is known that the innate immune system is activated by endogenous 'danger signals' such as tissue damage that involves necrotic cell death [14]. Indeed, titers of anti-FVIII inhibitory antibodies of the mice were elevated up to 400 BU mL^{-1} after the fifth intermittent stimulation of FVIII, in good agreement with previous findings [9]. Central VADs are associated with infectious and thrombotic complications necessitating the removal [6], although recent data from the international-ITI study showed that infectious episodes during ITI may not influence treatment outcome [15]. In our animal models, one mouse that had been frequently administered 0.05 U g^{-1} BW of FVIII exhibited a catheter-related bleeding (Fig. 2; LD#3), whereas another one with 0.5 U g^{-1} BW of FVIII had occlusion of iVAD system (Fig. 2, HD#4). Nonetheless, the iVAD would be a useful tool to evaluate immune response against sequential infusion of FVIII antigen in haemophilia A mice because they could be repeatedly infused more than 180 times over 50 weeks.

Recent study showed that port systems are suitable for inhibitor-expressing children with good predictors of ITI success [16,17]. In our murine model, high titers against FVIII (>2000 BU mL^{-1} during 50–100 EDs) were decreased to <500 BU mL^{-1} after 130–150 EDs in all

mice with serial infusion of 0.05 U g^{-1} BW of FVIII, even though they were continually exposed to FVIII antigen (Fig. 2). In contrast, mice administered high-dose 0.5 U g^{-1} BW FVIII five times a week had high titers of anti-FVIII inhibitory antibodies over 180 EDs, suggesting that dose of FVIII antigen might be crucial for the immune response in haemophilia A mice. We could not induce immune tolerance in any adult haemophilia A mouse with sequential infusion of FVIII antigen, according to the international consensus in which successful immune tolerance induction in haemophilia A is currently defined as both an undetectable inhibitor titer (less than or equal to 0.6 BU mL^{-1}) and normalized FVIII pharmacokinetics [18]. However, anti-FVIII IgG titers were markedly decreased to undetectable levels after 80–180 EDs in mice with serial infusion of 0.05 U mL^{-1} FVIII (Fig. 3). The discrepancy between anti-FVIII inhibitory titers and anti-FVIII IgG titers may be dependent on assay methods in which the former was one-stage APTT measurement and the latter was ELISA using an anti-FVIII monoclonal antibody as standard.

In haemophilia A patients, several researchers reported that IgG4 is the major component of anti-FVIII antibodies, although all IgG subclasses have been found [19,20]. In murine models, we showed that kinetics of anti-FVIII IgG1, IgG2a and IgG2b titers of haemophilia A mice with serial infusion of 0.05 U g^{-1} BW FVIII were similar to those administered 0.5 U g^{-1} BW FVIII (Fig. 4). In contrast, titers of anti-FVIII IgG3 subclass were decreased after 50–100 EDs in mice with serial infusion of 0.05 U g-1 BW FVIII. The Th1 immune response is believed predominant in patients with inhibitors in the long term [21], and was also the predominant response in mice that developed antibodies after challenge in adulthood [22,23]. We demonstrated a dose-dependent $CD4^+$ T-cell proliferative response to FVIII in preimmunized mice (five times injection of FVIII every 2 weeks), which is compatible with previous studies demonstrating that human FVIII is highly immunogenic in haemophiliac mice (Fig. 5) [24]. Interestingly, we observed that haemophilia A mice with sequential infusion of 0.05 U g^{-1} BW FVIII after 180 EDs failed to develop $CD4^+$ T-cell proliferative response to *in vitro* stimulation of FVIII antigen (Fig. 5). These T cells could not produce any IL-2, IL-4, IL-10, nor IFN-γ (Fig. 6), whereas those from mice immunized with five-times infusion of 0.5 U g^{-1} BW FVIII were able to secrete significant amounts of IL-2, IL-12 and IFN-γ. It is known that Th1 cells are initiators of antibody responses, and that they participate in class switching by releasing IFN-γ, which preferentially induces IgG2a and IgG3 in mouse [25]. Consequently, the FVIII-specific Th1 cytokine response may be partially suppressed by serial administration of FVIII in haemophilia A mice with inhibitors.

Several potential mechanisms of ITI have been identified [26]. These include clonal deletion (i.e. removal of immune-response cells through programmed cell death or apoptosis), anergy (failure of immune cells to respond to the FVIII molecule), or ignorance (i.e. the immune-response cells are 'blind' to the presence of FVIII). Our data suggest that sequential exposure of FVIII antigen could partially block anti-FVIII inhibitory antibody production, inducing T-cell anergy in haemophilia A mice with inhibitor, although our murine ITI model against heteroantibodies is fundamentally different from human ITI therapy against alloantibodies. However, further evaluation using completely continuous infusion system for the exposure of FVIII antigen will be necessary to confirm its efficacy in inducing immune tolerance [27]. Furthermore, understanding of the underlying mechanisms of immune tolerance induced by serial administration of FVIII is essential for the development of this strategy for haemophilia A patients with inhibitors.

Acknowledgement

We thank D.V.M. Hisae Yamauchi, D.V.M. Akane Hirosawa and Ms. Chizuko Nakamikawa for their excellent technical assistance. This work was supported in part by a Grant-in-Aid for Scientific Research (#19591133, #20591155, #21790920 and #21591249) from the Ministry of Education, Culture, Sports, Science and Technology, and by a Health and Labor Sciences Research Grant for Research from the Ministry of Health, Labor and Welfare, by Support Program for Strategic Research Platform, Baxter Hemophilia Scientific Research & Education Fund, and by JKA promotion funds from KEIRIN RACE.

Author contributions

SM designed and performed the research, analyzed data and wrote the paper; EK, YK, AY and AS performed experiments; SM, TO, JM and YS analyzed data and revised the paper.

Disclosures

The authors stated that they had no interests which might be perceived as posing a conflict or bias.

References

1 Hoyer LW. Hemophilia A. *N Engl J Med* 1994; 330: 38–47.
2 Ehrenforth S, Kreuz W, Scharrer I *et al.* Incidence of development of factor VIII and factor IX inhibitors in haemophiliacs. *Lancet* 1992; 339: 594–8.
3 Hoyer LW. Why do so many haemophilia A patients develop an inhibitor? *Br J Haematol* 1995; 90: 498–501.
4 Kreuz W, Becker S, Lenz E *et al.* Factor VIII inhibitors in patients with hemophilia A: epidemiology of inhibitor development and induction of immune tolerance for factor VIII. *Semin Thromb Hemost* 1995; 21: 382–9.
5 Ewenstein BM, Valentino LA, Journeycake JM *et al.* Consensus recommendations for use of central venous access devices in haemophilia. *Haemophilia* 2004; 10: 629–48.
6 Valentino LA, Ewenstein B, Navickis RJ, Wilkes MM. Central venous access devices in haemophilia. *Haemophilia* 2004; 10: 134–46.

7 Santagostino E, Mancuso ME. Venous access in haemophilic children: choice and management. *Haemophilia* 2010; 16(Suppl 1): 20–4.

8 Bi L, Lawler AM, Antonarakis SE, High KA, Gearhart JD, Kazazian HH Jr. Targeted disruption of the mouse factor VIII gene produces a model of haemophilia A. *Nat Genet* 1995; 10: 119–21.

9 Madoiwa S, Yamauchi T, Hakamata Y *et al.* Induction of immune tolerance by neonatal intravenous injection of human factor VIII in murine hemophilia A. *J Thromb Haemost* 2004; 2: 754–62.

10 Brackmann HH. Induced immunotolerance in factor VIII inhibitor patients. *Prog Clin Biol Res* 1984; 150: 181–95.

11 Nilsson IM, Berntorp E, Zettervall O. Induction of immune tolerance in patients with hemophilia and antibodies to factor VIII by combined treatment with intravenous IgG, cyclophosphamide, and factor VIII. *N Engl J Med* 1988; 318: 947–50.

12 Liesner RJ, Vora AJ, Hann IM, Lilleymann JS. Use of central venous catheters in children with severe congenital coagulopathy. *Br J Haematol* 1995; 91: 203–7.

13 Santagostino E, Gringeri A, Muca-Perja M, Mannucci PM. A prospective clinical trial of implantable central venous access in children with haemophilia. *Br J Haematol* 1998; 102: 1224–8.

14 Kono H, Rock KL. How dying cells alert the immune system to danger. *Nat Rev Immunol* 2008; 8: 279–89.

15 DiMichele DM, Goldberg I, Foulkes M, Hay RM. International prospective randomized immune tolerance (ITI) study: preliminary results of therapeutic efficacy and safety. *Haemophilia* 2010; 16(Suppl 4): 29.

16 DiMichele DM, Hoots WK, Pipe SW, Rivard GE, Santagostino E. International workshop on immune tolerance induction: consensus recommendations. *Haemophilia* 2007; 13(Suppl 1): 1–22.

17 Mancuso ME, Mannucci PM, Sartori A, Agliardi A, Santagostino E. Feasibility of prophylaxis and immune tolerance induction regimens in haemophilic children using fully implantable central venous catheters. *Br J Haematol* 2008; 141: 689–95.

18 Astermark J, Morado M, Rocino A *et al.* Current European practice in immune tolerance induction therapy in patients with haemophilia and inhibitors. *Haemophilia* 2006; 12: 363–71.

19 Fulcher CA, de Graaf Mahoney S, Zimmerman TS. FVIII inhibitor IgG subclass and FVIII polypeptide specificity determined by immunoblotting. *Blood* 1987; 69: 1475–80.

20 Gilles JG, Arnout J, Vermylen J, Saint-Remy JM. Anti-factor VIII antibodies of hemophiliac patients are frequently directed towards nonfunctional determinants and do not exhibit isotypic restriction. *Blood* 1993; 82: 2452–61.

21 Reding MT, Lei S, Lei H, Green D, Gill J, Conti-Fine BM. Distribution of Th1- and Th2-induced anti-factor VIII IgG subclasses in congenital and acquired hemophilia patients. *Thromb Haemost* 2002; 88: 568–75.

22 Wu H, Reding M, Qian J *et al.* Mechanism of the immune response to human factor VIII in murine hemophilia A. *Thromb Haemost* 2001; 85: 125–33.

23 Sasgary M, Ahmad RU, Schwarz HP, Turecek PL, Reipert BM. Single cell analysis of factor VIII-specific T cells in hemophilic mice after treatment with human factor VIII. *Thromb Haemost* 2002; 87: 266–72.

24 Qian J, Borovok M, Bi L, Kazazian HH Jr, Hoyer LW. Inhibitor antibody development and T cell response to human factor VIII in murine hemophilia A. *Thromb Haemost* 1999; 81: 240–4.

25 Stavnezer J. Immunoglobulin class switching. *Curr Opin Immunol* 1996; 8: 199–205.

26 Behrmann M, Pasi J, Saint-Remy JM, Kotitschke R, Kloft M. Von Willebrand factor modulates factor VIII immunogenicity: comparative study of different factor VIII concentrates in a haemophilia A mouse model. *Thromb Haemost* 2002; 88: 221–9.

27 Abe C, Tashiro T, Tanaka K, Ogihara R, Morita H. A novel type of implantable and programmable infusion pump for small laboratory animals. *J Pharmacol Toxicol Methods* 2009; 59: 7–12.

Cancer Research

NF-κB Activity Regulates Mesenchymal Stem Cell Accumulation at Tumor Sites

Ryosuke Uchibori[1], Tomonori Tsukahara[1], Hiroyuki Mizuguchi[4], Yasushi Saga[2], Masashi Urabe[1], Hiroaki Mizukami[1], Akihiro Kume[1], and Keiya Ozawa[1,3]

Abstract

Mesenchymal stem cells (MSC) accumulate at tumor sites when injected into tumor-bearing mice, perhaps offering cellular vectors for cancer-targeted gene therapy. However, the molecular mechanisms involved in MSC targeting the tumors are presently little understood. We focused on MSC–endothelial cell (EC) adhesion following TNF-α stimulation in an attempt to elucidate these mechanisms. Interestingly, stimulation of MSCs with TNF-α enhanced the adhesion of MSCs to endothelial cells *in vitro*. This adhesion was partially inhibited by blocking antibodies against vascular cell adhesion molecule-1 (VCAM-1) and very late antigen-4 (VLA-4). It is well known that TNF-α induces VCAM-1 expression via the NF-κB signaling pathway. Parthenolide has an anti-inflammatory activity and suppressed NF-κB activity by inhibition of IκBα phosphorylation after TNF-α stimulation and strongly inhibited TNF-α–induced VCAM-1 expression on MSCs. *In vivo* imaging using luciferase-expressing MSCs revealed that the bioluminescent signal gradually increased at tumor sites in mice injected with untreated MSCs. In contrast, we observed very weak signals at tumor sites in mice injected with parthenolide-treated MSCs. Our results suggest that NF-κB activity regulates MSC accumulation at tumors, by inducing VCAM-1 and thereby its interaction with tumor vessel endothelial cells. These findings have implications for the ongoing development of efficient MSC-based gene therapies for cancer treatment. *Cancer Res; 73(1); 364–72. ©2012 AACR.*

Introduction

Mesenchymal stem cells (MSC) are nonhematopoietic stem cells with high-proliferative potency and have the ability to differentiate into multiple lineages. They are detected in several adult and fetal tissues, including bone marrow, adipose tissue, and umbilical cord blood. MSCs have generated a great deal of interest in their potential use in regenerative medicine due to their ability to migrate to damaged tissues and to produce cytokines. Furthermore, MSCs can be easily genetically modified with viral vectors to be used as novel cellular vehicles in gene therapy protocols. MSCs are also used to treat severe acute GVHD, because they accumulate at inflammatory lesions and have immunomodulatory activity.

Interestingly, recent studies indicated that MSCs also have the ability to accumulate in tumors. Therefore, they can be used as cellular vehicles for cancer-targeted gene therapy. Intravenous injection of engineered MSCs expressing IFN-β was reported to inhibit the growth of melanoma pulmonary metastasis (1) and breast cancer (2) in mice and also prolonged the survival of mice with glioma xenografts (3). Furthermore, interleukin (IL)-12, which improves immune surveillance against cancer cells (4), and chemokine CX3CL1 (fractalkine), which is able to activate T cells and natural killer (NK) cells (5), were used as therapeutic molecules. We have also shown that retrovirus vector–producing MSCs also effectively inhibit tumor growth (6). In this context, treatment has been developed using retroviral vectors expressing the thymidine kinase of herpes simplex virus combined with the prodrug ganciclovir.

The ability of MSCs to specifically localize the multiple tumors, makes them extremely attractive for targeted cancer therapy. The most likely cause of preferential migration was considered to be the release of chemotactic gradients from tumor tissues. MSCs have a variety of chemokine and cytokine receptors and respond functionally to ligands *in vitro*. Tumors are known to produce a large amount of chemokines and cytokines, which could serve as ligands for the receptors on MSCs (7). Therefore, the mechanism of MSC accumulation at the site of tumors seems to be based on their migratory ability. Nevertheless, although various growth factors and chemokines, such as platelet-derived growth factor (PDGF), hepatocyte growth factor (HGF), and stromal cell–derived factor-1α (SDF-1α) may be involved, the detailed molecular mechanisms of MSC accumulation at tumors are poorly understood.

Authors' Affiliations: [1]Division of Genetic Therapeutics, Center for Molecular Medicine; [2]Department of Obstetrics and Gynecology; [3]Division of Hematology, Department of Medicine, Jichi Medical University, Tochigi; and [4]Department of Biochemistry and Molecular Biology, Osaka University, Osaka, Japan

Note: Supplementary data for this article are available at Cancer Research Online (http://cancerres.aacrjournals.org/).

Corresponding Author: Keiya Ozawa, Division of Genetic Therapeutics, Center for Molecular Medicine, Jichi Medical University, 3311-1 Yakushiji, Shimotsuke, Tochigi 329-0498, Japan. Phone: 81-285-58-7402; Fax: 81-285-44-8675; E-mail: kozawa@jichi.ac.jp

doi: 10.1158/0008-5472.CAN-12-0088

In the present study, we focused on MSC–endothelial cell (EC) adhesion following TNF-α stimulation in an attempt to elucidate the mechanism of MSC accumulation at tumors.

Materials and Methods

Cell culture

Bone marrow–derived human MSCs (Lonza Walkersville, Inc.) were cultured in mesenPRO RS medium (Invitrogen). HEK293-derived AD-293 cells (Stratagene), human embryonic fibroblasts WI-38 (RIKEN BRC), human colon adenocarcinoma cell lines SW480 (Cell Resource Center for Biomedical Research Institute of Development, Aging and Cancer, Tohoku University, Miyagi, Japan), and SW480/RFP that was generated by transduction of SW480 with red fluorescent protein-expressing retrovirus vectors (RV-RFP), were grown in Dulbecco's Modified Eagle's Medium (DMEM)/F-12 medium (Invitrogen) supplemented with 10% FBS, 100 U/mL penicillin, and 100 μg/mL streptomycin (P/S). Human endothelial progenitor cells (ApproCell Inc.) were cultured in endothelial progenitor cells grown medium (ApproCell Inc.). Human colon adenocarcinoma cell lines Colo205 (Cell Resource Center for Biomedical Research Institute of Development, Aging and Cancer Tohoku University) and Colo205/RFP that was generated by transduction with RV-RFP, were grown in RPMI medium (Invitrogen) supplemented with FBS and P/S. All cultures were kept in an incubator at 37°C and 5% CO_2.

Adenoviral vectors

Adenoviral vectors expressing a GFP were constructed by an improved *in vitro* ligation method (8, 9). The shuttle plasmid pHMCA5-GFP contains a CA promoter (a β-actin promoter/CMV enhancer with a β-actin intron), *GFP* gene, and a bovine growth hormone (BGH) polyadenylation signal, all of which are flanked by I-CeuI and PI-SceI restriction sites. I-CeuI/PI-SceI–digested pHMCA5-GFP was ligated with I-CeuI/PI-SceI–digested pAdHM4, resulting in pAdHM4-CAGFP. pAdHM41-K7-CAGFP was constructed by ligation of I-CeuI/PISceI–digested pHMCA5-GFP with I-CeuI/PI-SceI–digested pAdHM41-K7 (10). Viruses (Ad5-GFP and AdK7-GFP) were generated by transfection of PacI-digested pAdHM4-CAGFP and pAdHM41-K7-CAGFP, respectively, into AD-293 cells with SuperFect (Qiagen) according to the manufacturer's instructions. Each virus was purified by $CsCl_2$ step gradient ultracentrifugation followed by $CsCl_2$ linear gradient ultracentrifugation. Virus particles and biologic titers of each vector preparation were determined as described by Mittereder and colleagues (11). We also created Ad vectors expressing luciferase (Luc) using the shuttle plasmid pHMCA5-Luc, which contains the *Luc* gene derived from pELuc-test (Toyobo Co. Ltd.). MSCs and fibroblasts were seeded in culture plates or flasks at a density of 1×10^4 cells/cm^2, and the next day the cells were treated with each adenovirus vector for 1.5 hours. The medium containing the vectors was removed and replaced with fresh medium.

Animal models

All animal experiments were approved by the Jichi Medical University (Tochigi, Japan) ethics committee and carried out in accordance with the NIH Guide for the Care and Use of Laboratory Animals. To create tumor-bearing mice, SW480/RFP cells (3×10^6) were subcutaneously inoculated into 4- to 6-week-old male Balb/c nu/nu mice (Clea Japan Inc.). The mice were used for experiments 7 days after inoculation.

Immunohistochemistry

Cultured MSCs and fibroblasts were transduced with AdK7-GFP at a concentration of 3,000 virus particles per cell (vp/cell). Two days after transduction, cells were injected into the left ventricular cavities (1×10^6, day 0) of tumor-bearing mice. Mice were sacrificed on day 4, and 7-μm serial cryosections from frozen tissues were processed. Immunohistochemistry was conducted with fluorescein isothiocyanate (FITC)-conjugated anti-GFP antibody (ab6662; Abcam Inc.) on tumor cryosections to detect MSCs or fibroblasts. Nuclei were stained with 4′,6-diamidino-2-phenylindole (DAPI; Vector Laboratories, Inc.). Images were obtained with a fluorescence microscope (BZ-9000; Keyence). SW480/RFP cells (3×10^6) were subcutaneously inoculated into 4- to 6-week-old male Balb/c nu/nu mice. Mice were sacrificed on day 11, serial sections from tumor tissues were processed. Immunohistochemistry was conducted with anti-mouse CD34 monoclonal antibody (MEC14.7; GeneTex Inc.) on tumor section to detect tumor blood vessels. Histofine Simple Stain Mouse MAX PO (Nichirei Biosciences, Inc.) was used as a horseradish peroxidase–conjugated secondary antibody, and 3,3′-diaminobenzidine (DAB) solution was used for brown color development. Sections were then counterstained with Hematoxylin (Wako Pure Chemical Industries, Ltd.). Images were obtained with a fluorescence microscope (BZ-9000).

In vivo imaging of homing ability to tumors

Cultured MSCs and fibroblasts were transduced with AdK7-Luc at a concentration of 3,000 and 680 vp/cell, respectively. Two days after transduction, cells were injected into the left ventricular cavities (1×10^6, day 0) of tumor-bearing mice, and then optical bioluminescence imaging was conducted to periodically trace the cells using an *in vivo* imaging system (IVIS; Xenogen). To detect bioluminescence from MSCs or fibroblasts, the reporter substrate D-luciferin (Ieda Chemical Co., Ltd.) was injected into the mouse peritoneum (75 mg/kg body weight) for scanning. The luminescent intensity at tumor sites was analyzed using Living Image software (Xenogen).

In vitro migration assays

Cultured MSCs or fibroblasts were serum-starved for 12 hours. One hundred microliters of tumor conditioning medium (CM), or serum-free medium supplemented with PDGF-BB (10 ng/mL), HGF (30 ng/mL), fibroblast growth factor-β (FGF-β; 20 ng/mL), SDF-1α (150 ng/mL), VEGF-A (25 ng/mL), or monocyte chemoattractant protein-1 (MCP-1; 100 ng/mL) was added to the lower wells of migration chambers (8-μm pore size; Neuro Probe, Inc.); MSCs or fibroblasts (4×10^4) were added to the upper wells. All recombinant proteins were purchased from R&D systems Inc.. Medium alone (DMEM/F-12) was used as a negative control and treatment with 30% FBS was the positive control. After incubation for 24 hours at

37°C, cells were labeled with CyQUANT NF dye, and cells attached to the lower surface of the filters were detached with trypsin. Fluorescent intensity was measured using a fluoroscan, and the number of adherent cells was quantified using a standard curve constructed by a known number of cells.

Flow cytometric analysis of adhesion molecules

Cultured MSCs, fibroblasts or endothelial cells were stimulated with TNF-α and harvested by trypsinization. Cell aliquots were incubated with FITC-conjugated monoclonal antibodies (BD) against vascular cell adhesion molecule-1 (VCAM-1), CD49d, CD29 (Integrin-β1), and analyzed by flow cytometry (FACScan; BD Biosciences). For each analysis, an aliquot of cells was also stained with isotype control immunoglobulin G (IgG)–conjugated to FITC as a negative control.

Assay for TNF-α produced in tumor-bearing mice

SW480/RFP (3×10^6) cells were subcutaneously inoculated into nude mice. Seven days after inoculation, mice were anesthetized with an overdose of isoflurane inhalation. The blood was collected and allowed to coagulate overnight on ice. After centrifugation of the samples (2,000 × *g*, 30 minutes, 4°C), the serum was removed and stored at −70°C. Tumor, spleen, and liver tissues were homogenized in 1.5 mL of α-minimum essential medium using a tissue homogenizer. The homogenates were then centrifuged (2,000 × *g*, 30 minutes, 4°C), and the supernatant was removed and recentrifuged (14,000 × *g*, 30 minutes, 4°C). Serum and supernatants from tissue homogenates were kept at −70°C until use. TNF-α was assayed using a commercially available ELISA kit (mouse TNF-α Instant ELISA; Bender MedSystems) according to the manufacturer's protocols.

***In vitro* adhesion assays**

For adhesion assays, endothelial cells (at 4 passages) were cultured to confluence on fibronectin-coated 96-well plates (20 ng/mL; Sigma-Aldrich, Inc.) and treated with TNF-α (10 ng/mL) for 12 hours before assaying. MSCs and fibroblasts were treated with TNF-α (10 ng/mL) 12 hours before the adhesion assays and incubated with isotype control IgG or anti-VCAM-1 or very late antigen-4 (VLA-4; 10 μg/mL) monoclonal antibodies (mAb) for 1 hour. Cells were labeled with CyQUANT NF dye, and 1×10^4 cells were seeded onto endothelial cells. After 30 minutes of incubation at 37°C, wells were washed thoroughly 3 times with PBS to remove nonadherent cells. Fluorescent intensity was measured using a fluoroscan, and the number of adherent cells was quantified using a standard curve constructed by a known number of cells. In some experiments, MSCs and fibroblasts were pretreated for adhesion studies with one of the following substances: TNF-α (10 ng/mL), anti-VCAM-1 antibody (mouse monoclonal anti-rat, clone 5F10, 10 μg/mL, Eurogentec), or anti-VLA-4 antibody (mouse monoclonal anti-rat, clone 1A29, 10 μg/mL, Research Diagnostics).

Parthenolide treatment of MSCs

Parthenolide (Biomol) was reconstituted in dimethyl sulfoxide (DMSO; Sigma-Aldrich, Inc.) to a stock concentration of 0.4 mol/L and subsequently diluted in PBS. MSCs were treated with parthenolide (5 μmol/L) for 6 hours before experiments. To assess the effect of parthenolide treatment of transgene expression, cells were reseeded into 96-well plates, and luciferase assays were conducted using luciferase-expressing MSCs. Cell viability after parthenolide treatment was also examined with Cell Proliferation Kit II [2,3-bis[2-methoxy-4-nitro-S-sulfophenynl]H-tetrazolium-5 carboxanilide inner salt (XTT); Roche Diagnostics GmbH] according to the manufacturer's instructions.

Western blotting

Western blot analysis was conducted to measure the NF-κB pathways. Next, MSCs were pretreated with parthenolide or vehicle (DMSO) for 6 hours, and then cultured with TNF-α (10 ng/mL) for 3 minutes. Cells were lysed in radioimmunoprecipitation assay (RIPA) buffer containing protease inhibitor (Pierce Biotechnology). Protein extracts were electrophoresed on a 4% to 12% Bis–Tris gel (Invitrogen), and transferred to polyvinylidene difluoride (PVDF) membranes. Membranes were incubated in PVDF blocking reagent (TOYOBO), and then incubated with primary antibodies against the following proteins: IκBα, phospho-IκBα (Ser32), NF-κB p65, phospho-NF-κB p65 (Ser536), and α-tublin (Cell Signaling Technology), followed by incubation with horseradish peroxidase-conjugated goat anti-rabbit IgG or -mouse IgG1 secondary antibody, and detected using a Western blotting detection system (GE Healthcare).

Immunocytochemistry

To visualize p65 nuclear translocation, MSCs were pretreated with parthenolide or vehicle (DMSO) for 6 hours and then cultured with TNF-α (10 ng/mL) for 20 minutes. Cells were fixed with 4% fomaline and permiabilized with Triron-X 100. After washing with PBS, slides were incubated with rabbit anti-p65 antibody (Cell Signaling Technology), followed by incubation with Alexa Fluor 488–conjugated goat anti-rabbit IgG secondary antibody. The actin cytoskeleton was stained with Alexa Fluor 546–conjugated phalloidin (Invitrogen); nuclei were stained with 1,5-bis{[2-(di-methylamino) ethyl]amino}-4,8-dihydroxyanthracene-9,10-dione (DRAQ)-5 dye (Invitrogen). Cells were examined using Keyence BZ-9000.

Results

***In vivo* imaging of MSC accumulation in tumors**

We used bone marrow–derived human MSCs, which expressed characteristic phenotypic markers for MSCs and differentiated into adipocyte, osteocyte, and chondrocyte under specific culture conditions (Supplementary Fig. S1). Then, fiber-modified adenovirus vectors (AdK7) were used for efficient transduction of MSCs and fibroblasts in this study. When the cells were transduced with GFP-expressing AdK7 vectors at a density of 3,000 vp/cell, transduction efficiency was almost 100% (Supplementary Fig. S2A and S2B). The bioluminescent intensity of MSCs transduced with luciferase-expressing Ad vectors at 3,000 vp/cell was equal to that of fibroblasts transduced at 680 vp/cell (Supplementary Fig. S2C). Mice injected with GFP-expressing MSCs or fibroblasts were sacrificed 4 days after injection for immunohistochemical analysis.

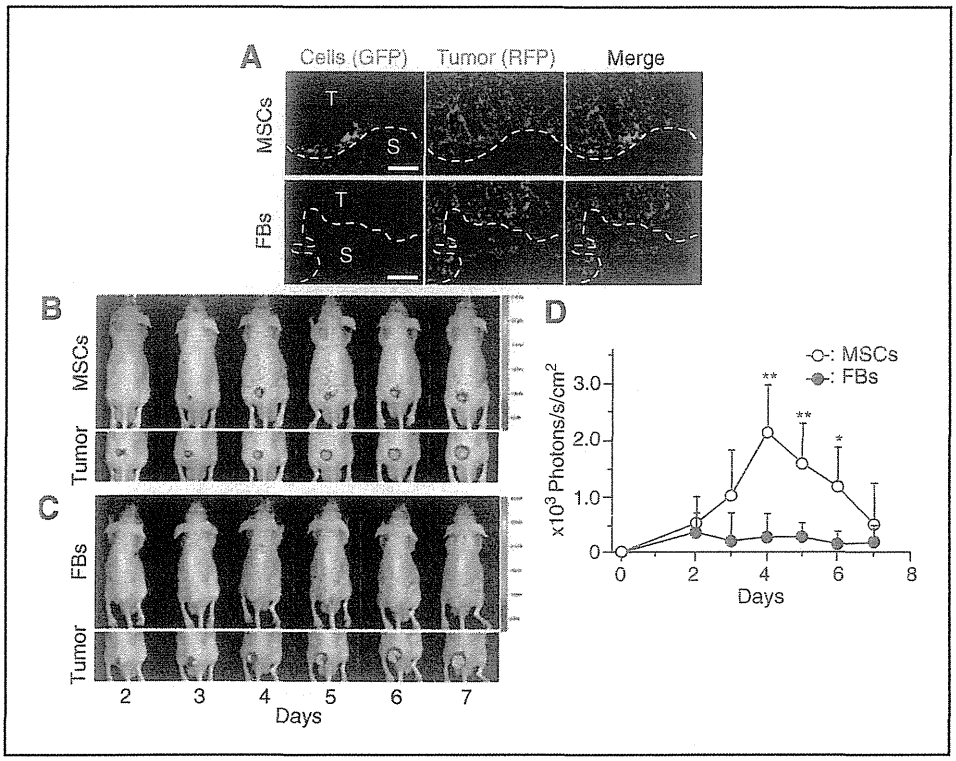

Figure 1. Tumor homing ability of MSCs *in vivo*. A, subcutaneous tumors were induced by injection of SW480/RFP cells (3×10^6) in nude mice (day 0). Cultured MSCs or fibroblasts were transduced with GFP-expressing adenovirus vectors 2 days before injection (day 5) and were injected into the left ventricular cavity (1×10^6, day 7). Mice were sacrificed on day 11, and immunohistochemistry was conducted with anti-GFP antibody on tumor cryosections to detect MSCs or fibroblasts. Top, fluorescent microscopy view of MSC detection; MSCs (left), RFP-labeled tumor cells (center), nucleic staining with DAPI and merge (right). Bottom, fluorescent microscopy view of fibroblast detection; fibroblasts (left), RFP-labeled tumor cells (center), nucleic staining with DAPI and merge (right). Data shown are from 1 representative experiment of 3 carried out. Scale bar, 100 μm. S, stroma; T, tumor. B, luciferase-expressing MSCs were injected into tumor-bearing mice via the left ventricular cavity (1×10^6, day 7). Optical bioluminescence imaging was conducted to periodically trace the cells using IVIS. Top, biodistribution of MSCs as detected by luminescence. Bottom, tumor site detected by red fluorescence. Data shown are from 1 representative experiment of 8 carried out. C, luciferase-expressing fibroblasts were injected into tumor-bearing mice and IVIS imaging was conducted as described earlier. Top, biodistribution of fibroblasts indicated by luminescence. Bottom, tumor site indicated by red fluorescence. Data shown are from 1 representative experiment of 7 carried out. D, bioluminescent intensity at tumor sites was quantified using analysis software. The data are expressed as mean ± SD ($n = 8$ for MSCs and $n = 7$ for fibroblasts). *, $P < 0.05$; **, $P < 0.01$ compared with fibroblasts at the same time.

MSCs identified with anti-GFP antibody were detected in the boundaries of tumors and tumor stroma. However, we found no GFP-positive fibroblasts in the tumor tissues (Fig. 1A). We also used bioluminescence imaging to quantitatively investigate the tumor tropism of MSCs. We injected luciferase-expressing MSCs or fibroblasts into mice through the left ventricular cavity, and then conducted optical bioluminescence imaging to periodically trace the cells using IVIS. In mice injected with luciferase-expressing MSCs, optical bioluminescence at tumor sites became pronounced over time (Fig. 1B), and signal intensity gradually increased (Fig. 1D). In contrast, we observed no signal at the tumor sites in mice injected with luciferase-expressing fibroblasts (Fig. 1C and D).

In vitro migration assays

We analyzed the effects of several growth factors (specifically PDGF-BB, HGF, and VEGF), chemokines (specifically MCP-1 and SDF-1α), and SW480 culture–conditioned medium on MSC and fibroblast migration. These factors are commonly expressed in tumor tissues, and are thought to be potential mediators of MSC tropism. We also used serum-free medium as a negative control and medium containing 30% FBS as a positive control. Migration was quantified by direct labeling and counting of cells by a fluorometer (Fluoroskan Ascent FL; Thermo Labsystems). Exposure to PDGF, HGF, or conditioned medium from SW480 cells stimulated significant MSC migration, whereas VEGF and SDF-1α had no significant effect as compared with serum-free medium (Fig. 2). We compared the migration capacity of MSCs and fibroblasts, the factors that attracted MSCs also induced migration of fibroblasts. Rather, it seems that fibroblasts were more strongly attracted to these factors than MSCs.

In vitro adhesion assays

The tumors generated in mice in this study strongly induced tumor stroma with defined blood vessels, and MSCs specifically accumulated in this stroma (Fig. 3A). Therefore, we propose a hypothesis as follows: factors, as indicated in Fig. 2, attract both MSCs and fibroblasts to the tumor microenvironment, but importantly, MSCs significantly adhere to endothelial cells as

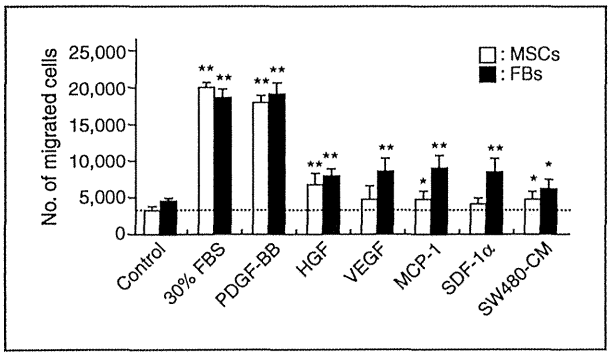

Figure 2. Migratory capacity of MSCs and fibroblasts (FB) in response to growth factors, chemokines, and conditioned medium from SW480 cells. MSCs or fibroblasts were serum-starved for 12 hours. Cells (4×10^4) were added to upper wells of migration chambers. Then, tumor conditioning medium, serum-free medium supplemented with PDGF-BB (10 ng/mL), HGF (30 ng/mL), SDF-1α (150 ng/mL), VEGF-A (25 ng/mL), or MCP-1 (100 ng/mL) were added to the lower wells. Treatment with medium alone (DMEM/F-12) was used as a negative control and treatment with 30% FBS was used as the positive control. The contents of the upper wells and lower wells were separated by polycarbonate filters (8 μm). The data are expressed as mean ± SD ($n = 8$ per cell type). Values are presented as mean ± SE. *, $P < 0.05$ and **, $P < 0.01$ compared with each control.

compared with fibroblasts. Therefore, only MSCs migrate and accumulate at tumor sites via blood vessels in tumor stroma. We speculated that inflammatory cytokines (specifically TNF-α) are required for induction of adhesion molecule expression. First, we measured TNF-α levels in tumor tissues by ELISA. The TNF-α level is significantly higher in tumor tissues as compared with liver and spleen (Fig. 3B). Similar results were also observed in another experiments using Colo205 tumor cells (Supplementary Fig. S3). Then, we assessed the expression of adhesion molecules on endothelial cells, MSCs, and fibroblasts by fluorescence-activated cell sorting analysis. After TNF-α stimulation, endothelial cells and MSCs significantly expressed adhesion molecules including VCAM-1 and VLA-4, compared with fibroblasts (Fig. 3C). We also examined the *in vitro* adhesion of MSCs to endothelial cells. MSCs effectively adhered to endothelial cells as compared with fibroblasts (Fig. 3D). Furthermore, this adhesion was partially inhibited by blocking antibodies against VCAM-1 and VLA-4.

Effects of parthenolide on MSC migration and adhesion

We propose a hypothesis that if TNF-α–induced VCAM-1 expression is inhibited, MSC accumulation at tumors is also attenuated. It is well known that TNF-α induces VCAM-1 expression through the NF-κB signaling pathway. We used parthenolide, a sesquiterpene lactone that occurs naturally in the Feverfew plant. Although parthenolide has several biologic activities, we focused on its suppressive effect on NF-κB activity. At first, there were no differences in migratory capacity toward growth factors or chemokines with or without parthenolide treatment (Fig. 4A). Next, we assessed the inhibitory effect of parthenolide on NF-κB activity: MSCs were pretreated for 6 hours, and then were stimulated with TNF-α for 3 minutes. Parthenolide suppressed p65 nuclear translocation through the inhibition of IκBα phosphorylation (Fig. 4B and C) and strongly inhibited the TNF-α–induced VCAM-1 expression on MSCs (Fig. 4D). Consequently, and MSC–EC adhesion was strongly inhibited by parthenolide treatment similarly to anti-VCAM-1 blocking antibody (Fig. 4E).

***In vivo* imaging of parthenolide-treated MSCs**

First, we examined the effect of parthenolide treatment on transgene expression and cell viability. There were no significant effects on transgene expression and cell viability after parthenolide treatment (Fig. 5A and B). Next, we conducted *in vivo* imaging using IVIS. We observed definite bioluminescence at tumor sites in the mice injected with untreated MSCs (Fig. 5C), and bioluminescent intensity was gradually increased (Fig. 5E), as indicated earlier (Fig. 1B). In contrast, we could not observe definite accumulation at the tumor sites in mice injected with parthenolide-treated MSCs (Fig. 5D and E). Similar results were also obtained by experiments using Colo205 tumor-bearing mice (Supplementary Fig. S4).

Discussion

In this study, we showed that MSC accumulation at tumor sites would be related not only to migratory capacity toward growth factors and chemokines, but also to MSC–EC adhesion following activation by TNF-α. We further showed that NF-κB activity regulates MSC accumulation at tumor sites through the induction of VCAM-1 expression and the resultant interaction with tumor blood vessel endothelial cells.

It is thought that MSCs are mobilized into action following tissue damage, such as injury or inflammation typically accompanied by the release of inflammatory cytokines from the damaged tissues, leading to the recruitment of MSCs to the target. Tumors have a microenvironment consisting of large numbers of inflammatory cells (12). This microenvironment promotes the recruitment of MSCs via various soluble factors secreted by the tumor and inflammatory cells, including EGF, VEGF-A, FGF, PDGF, SDF-1α, IL-8, IL-6, granulocyte colony-stimulating factor (G-CSF), granulocyte-macrophage colony-stimulating factor (GM-CSF), MCP-1, HGF, TGF-β1, and urokinase-type plasminogen activator (uPA; ref. 13). However, in our experimental settings, although systemically injected MSCs accumulated at the tumors, subcutaneously injected MSCs did not (data not shown). We also compared the migration capacity of MSCs and fibroblasts toward growth factors and chemokines *in vitro*. Rather, it seems that fibroblasts were more strongly attracted to these factors than MSCs. Our results suggest that the mechanism of MSC accumulation cannot be explained solely by cytokine-mediated migration. Therefore, we need different viewpoints to clarify the mechanism.

The tumors generated in this study strongly induced tumor stroma with large numbers of blood vessels, and MSCs in particular accumulated in the boundaries between the tumors and tumor stroma. Furthermore, MSC accumulation at the site of the tumors was observed only when cells were injected via the left ventricular cavity. Therefore, we focused on MSC–EC adhesion to elucidate the mechanisms involved.

It has previously been reported that the interaction of MSCs with the vascular endothelium resembles leukocyte chemotaxis (14). To analyze these interactions, we referred to a model